ABSTRACT

Title of Dissertation:	UNDERSTANDING CLIMATIC FACTORS DRIVING WILDFIRES IN THE WESTERN U.S.
	Lei Zhang, Doctor of Philosophy, 2024
Dissertation directed by:	Professor Zhanqing Li, Department of Atmospheric and Oceanic Science

Wildfires have profound and catastrophic impacts on landscapes and human society and act as important agents in the transformation of ecosystems. Over the past decades, the western United States (WUS) has experienced a significant increase of large wildfires, with substantial rise of the economic and ecological costs. Considerable research efforts towards understanding climate change as a primary driver of larger and more severe wildfires, which exacerbates summer drought, reduces spring snowpack, etc. However, the physical relationships among wildfires in North America (NA) and regional feedback processes to changes in the large-scale circulation, global dryness, and linkages to global warming are still poorly understood. Our observational analyses of wildfire-climate relationships in North America were conducted using diverse independent observations and reanalysis data sets for the period 1984–2014. Results show that the WUS has experienced the most robust increase in burned area. In addition to warming, the WUS has been under the influence of multi-decadal trends in

tropospheric relative humidity deficit, reduced cloudiness, increased surface net insolation, and enhanced adiabatic warming and drying from increased tropospheric subsidence, as well as drying from enhanced offshore low-level flow. These trends are found to be associated with a widening of the descending branch of the Hadley circulation, consistent with climate model projections under greenhouse gases warming. This work sheds new light on the underlying regional climate processes affecting wildfire trends in NA and linkages with climate change under global warming. My second work focuses on analyzing the causes of the exceptional 2020 fire season in the WUS. Our comprehensive examination shows this extraordinary year for fires in the WUS is the results of "perfect storm", a combination of multiple climate and weather extremes events. Extreme fuel aridity in September serves as a compelling example of the critical significance of tropospheric subsidence to the surface and atmospheric RH deficit. The third study evaluates performance of the Canada and US fire indices over the various ecoregions of the WUS. My study also finds Haines index combined with current index further improves the performance of conditional frequency distribution and predictive skill of large fires, suggesting the importance and merit of input from atmosphere dryness and stability into current fire indices.

UNDERSTANDING CLIMATIC FACTORS DRIVING WILDFIRES IN THE WESTERN U.S.

by

Lei Zhang

Dissertation submitted to the Faculty of the Graduate School of the
University of Maryland, College Park, in partial fulfillment
of the requirements for the degree of
Doctor of Philosophy
2024

Advisory Committee:
Professor Zhanqing Li, Chair
Senior Research Scientist William K.M Lau
Professor Rachel Pinker
Professor Ning Zeng
Professor Tatiana V Loboda

Dedication

To my dear parents Jun Zhang and Huiqin Zhu

For their unconditional love and support

Acknowledgements

First and foremost, I would like to express my deepest gratitude to my academic advisor, Distinguished Professor Zhanqing Li. Thank you for your invaluable support and patience throughout this long and precious journey. Words are inadequate to express my sincere gratitude to you.

I would also like to convey my profound appreciation to my research advisor, Dr. William K.M Lau, for your unwavering guidance and patience. Your insights and expertise have been instrumental in helping me shape this work. Thank you for your encouragement when I was lost in my research.

I am very grateful to my committee members, Dr. Ning Zeng, Dr. Rachel Pinker and Dr. Tatiana Loboda for your valuable suggestions on my dissertation.

Thanks to my colleague Dr. Weichen Tao. Thank you for your help and solutions when I had research problems. I would also Thank Ms. Maureen Cribb, for your assistance in proofreading my papers.

Special thanks to all my colleagues and friends during my time at College Park. Thank you all including Dr. Tianning Su, Dr. Xin Xu, Dr. Xiaoai Jin, Dr. Jing Wei, Haipeng Zhang, Siyu Shan, Dr. Tianmeng Cheng, Dr. Cheng Yuan, Dr. Chuchun Chang and Dr. Cheng Da.

Table of Contents

List of Tables

List of Figures

List of Abbreviations

AMO = Atlantic Multidecadal Oscillation
AK = Alaska
BI = Burning Index
BUI = Buildup Index
CO = Colorado
CA = California
CC = Clausius–Clapeyron
CG = Cloud-to-Gound
CFFDRS = Canadian Forest Fire Danger Rating System
DC =Drought Code
DMC =Duff Moisture Code
DTS = Deep Tropical Squeeze
dNBR = differenced Normalized Burn Ratio
ENSO = El Niño-Southern Oscillation
EPA = Environmental Protection Agency
ERC = Energy Release Component
FFMC = Fine Fuel Moisture Code
FWI =Fire Weather Index
GHG = Greenhouse Gas
GHCN2 = Global Historical Climate Network
HC = Hadley circulation
HDWI = Hot and Dry wind index
ICOADS = International Comprehensive Ocean-Atmosphere Data Set
IC = Ignition Component
ISCCP = International Satellite Cloud Climatology Project
ITCZ = Intertropical convergence zone
MTBS = Monitoring Trends in Burn Severity
MODIS = Moderate resolution imaging spectroradiometer
NA =North America
NLDN = National Lightning Detection Network
NFDB= National Fire Database
NFDRS = National Fire-Danger Rating System
NPSH = the North Pacific Subtropical High
OR=Oregon
PDO = Pacific Decadal Oscillation
PDSI = Palmer Drought Severity Index
RH = Relative humidity
RCFW = Regional climate feedback exacerbating wildfires SC = Spread Component
SC= Spread Component
SLP = Sea-level pressure
SRB = Surface Radiation Budget
SWDR = Shortwave downward radiation
VPD= vapor pressure deficit
WUS= western United States

Chapter 1: Introduction

1.1 Background

A widespread increase in fire activity has been well documented across North America in recent decades. Numerous studies have found significant increasing trends in occurrence, total burned area and duration of wildfires over western US, boreal region of Canada and Alaska (Dennison et al., 2014; Westerling et al., 2006). These increased fire activities in recent decades have been attributed to several major drivers, including anthropogenic climate change, natural climate variability and human suppression and settlement (Abatzoglou & Williams, 2016; Zhuang et al., 2021).

Climatic factors including warmer temperature, earlier snowing melting, reduced rainfall and increased lightning activities are believed to be key drivers contributing to the frequency, severity, and length of fires in North America (Higuera et al., 2021; Holden et al., 2018; Littell et al., 2016; Running, 2006; Veblen et al., 2000; Veraverbeke et al., 2017; Westerling et al., 2003, 2006). The trend of these factors is generally consistent with those expected from greenhouse gas (GHG) warming (Abatzoglou & Williams, 2016).

However, the trend could be confounded by large-scale mode of natural climate variability such as El Niño-Southern Oscillation (ENSO), the Pacific Decadal Oscillation (PDO) and Atlantic Multidecadal Oscillation (AMO), which affect winter temperature and precipitation regimes in western North America through mid-latitude teleconnections (Fasullo et al., 2018). Recent study shows the natural variability of atmospheric circulation contributes to one-third of the vapor pressure deficit (VPD)

trend based on an ensemble constructed flow analogue approach (Zhuang et al. 2021). In addition, land cover change, ignitions and fire suppression further complicate the fire activity varying greatly across space and time. Recent study shows human-started wildfires accounts for 84% of all wildfires, triple the length of the fire season and responsible for nearly half of all areas burned over contiguous US (Bach et al. 2016).

Despite of these complicated and intertwined factors, anthropogenic climate change, the impact of anthropogenic climate change on fire weather is emerging above natural variability by recent observation and modelling studies over global (Jolly et al. 2015). Substantial increases of extreme fire weather occurred over a quarter to almost half of the global burnable land driven by atmospheric humidity and temperature (Jain et al. 2022). For western US and Canada, the impacts of anthropogenic climate change on fire weather extremes and fire season length emerged in the 2010s (Abatzoglou et al., 2019; Williams et al., 2019; Abatzoglou & Williams, 2016). The occurrence of extreme fire risk would exceed natural variability in California by 2020 (Yoon et al 2015). It is anticipated that extraordinary fire seasons, such as that of 2020, will become more common, and that future extreme wildfire events will surpass any previously recorded levels (Coop et al. 2022).

1.2 Gaps in the existing works

Climatic explanations posit that recent increases in western US wildfire activity are related to three hypothesized climatic drivers: decreased snowpack, increased temperature, and decreased precipitation (Holden et al., 2018; Westerling et al., 2006). The most cited hypothesis is the early winter snowmelt regulating western US fire activity. In western mountains, snow carries over a large portion of winter precipitation

and releases it gradually in late spring and early summer. The earlier snowmelt could lead to a longer and earlier dry season and strongly associated with drying of soils and vegetation, providing greater danger of large fires. Temperature hypothesis is that increased surface air temperature affects summer drought and vapor pressure deficit (VPD), thus flammability of fuels in forests and wildfire activity. The third hypothesis indicates that decreased summer precipitation and wetting rain days have likely been a primary driver of increases in wildfire area burned in western US as an additional mechanism during the past three decades. While there is little doubt that warming temperature, decreasing snowpack and summer rainfall play important roles in promoting recent forest fire in North America, treating the temperature, VPD and precipitation effects in isolation could ignore the potential hydrologic feedback, which are driven by warm season moisture variations. Few studies have linked these different climate elements together, and the importance of tropospheric drying to wildfire is mostly overlooked. Previous modeling studies indicate that meteorological droughts over the US maybe a component of a canonical response of a global precipitation pattern to global warming, linked to a large-scale overall reduction in relative humidity (RH) in the mid and lower troposphere of the subtropics (Lau & Kim, 2015 Fig1.1) , and the long-term structural changes in the intertropical convergence zone (ITCZ) and associated precipitation–radiation–circulation feedback processes are examined using multiple sources of reanalysis data (Lau and Tao,2020). However, no previous study has explored the physical mechanism linking wildfires in North America and regional feedback processes to changes in the large-scale circulation, global dryness, and linkages to GHG-induced warming. This gap of understanding between wildfire,

atmospheric drying, Change of Hadley circulation in a warming world motivate me to seek observational evidence of these linkages, which will be illustrated in Chapter 2.

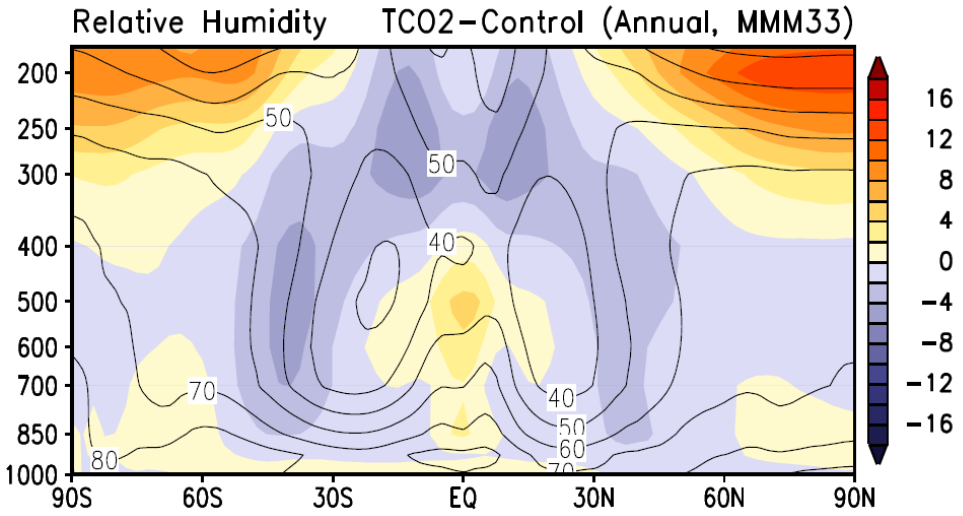

Fig 1.1 Changes in tropospheric RH projected by CMIP5 models under a scenario of1% per year increased CO2. Adopted from Lau and Kim (2015)

1.3 Objective

The overall goal of my dissertation is to achieve a better understanding of what climate factors and mechanisms drive the increasing wildfire activities in North America. To address this scientific question, the dissertation gives a comprehensive and in-depth exploration of the relationships among the elements of the atmospheric water cycle, surface process and wildfire by utilization of ground and satellite observations, reanalysis data and machine learning modelling. Three specific questions we are trying to answer: (1) What are the relationships between wildfire and climate variables in North America, and how are they connected under the greenhouse gas warming? (2) what is the possible explanation and causes for the devastating western U.S wildfire season in 2020? (3) How the Canada and US fire indices compared over the different ecoregions over western U.S and any improvement for the current indices.

1.4 Dissertation Structure

The first chapter provides an overall introduction of background and motivation in this dissertation. The major research objectives and questions are also introduced in this chapter. Three research chapters are followed, and the last chapter is a conclusion and future work.

Chapter 2 addresses the science question 1 by exploring the physical relationships among wildfires in North America and regional feedback processes to changes in the large-scale circulation, global dryness, and linkages to GHG-induced warming. Multiple source evidence of surface and satellite observations, together with five reanalysis data are provided to reveal these relationships and shew new light on the underlying regional climate processes affecting wildfire trends in North America. This work has been peer reviewed and published in *Geophysical Research Letters* (Zhang et al. 2020). Chapter 3 focuses on science question 2, which investigates the climate impact and possible causes for the extraordinary 2020 western U.S. fire season. The record-setting atmospheric dryness across much of the western US plays a major role in this year's anomalous fire activity. The anomalous dryness could be a combination consequence of global warming, natural variability and local wildfire-climate feedback as we discussed in Chapter 2. Chapter 4 evaluates the different fire indices from Canada and US fire danger rating system over the various ecoregions of the western U.S. and develop a new combined index with lower atmospheric stability (Haines index). As noted above, Chapter 5 presents the overall conclusions of this doctoral research, potential future research topics and implications resulting from the current research.

Chapter 2: Large wildfires in the western United States exacerbated by tropospheric drying linked to a multi-decadal trend in the expansion of the Hadley circulation

2.1 Introduction

Staggering socioeconomic losses stemming from more frequent and severe wildfires in North America in recent decades have drawn much attention to the need for better understanding the causes of increased wildfires, in order to inform and provide sound strategies for mitigation. Numerous studies have found significant increasing trends in occurrence, total burned area, and duration of wildfires in the western United States, most pronounced in the forests of the northern U.S. Rocky Mountains (Dennison et al., 2014; Westerling et al., 2006). Burned areas of large fires have doubled in the boreal region of Canada and Alaska from 1959 to 1999 (Kasischke & Turetsky, 2006). These increased wildfire activities have been linked to natural climate variability and human activities (Abatzoglou & Williams, 2016; Balch et al., 2017; Harvey, 2016; Littell et al., 2009). Warmer temperatures, earlier snowing melting, prolonged summer droughts, vegetation type, and increased lightning are believed to be key factors contributing to the frequency, severity, and length of wildfires (Holden et al., 2018; Littell et al., 2016; Running, 2006; Veblen et al., 2000; Veraverbeke et al., 2017; Westerling et al., 2003, 2006). These studies and others have led to the following assessment statement (Wuebbles, 2017): "The incidence of large forest fires in western United States and Alaska has increased since the early 1980 (high confidence) and is projected to further increase in those regions as the climate warms with profound change to certain ecosystems (medium confidence)."

Contemporaneously, there have also been multiple lines of evidence indicating that greenhouse-gas (GHG)-induced global warming may have increased droughts over the globe during recent decades (Dai et al., 2004; Dai, 2006, 2011; Dai & Zhao, 2017), together with the expansion of semiarid and desert regions (Huang et al., 2016). Such a global drying trend is projected to worsen in the future, mainly due to an increased water vapor deficit (Dai, 2013; Dai et al., 2018; Feng & Fu, 2013; Lau & Kim, 2015; Zhao & Dai, 2017). Previous studies suggest that the impact of anthropogenic climate change on fire weather is emerging above natural variability in NA (Abatzoglou et al., 2019; Kirchmeier-Young et al., 2017). For western U.S., two thirds of the increasing VPD are likely due to anthropogenic warming based on an ensemble constructed flow analogue approach (Zhuang et al., 2021). It is important to stress that the trend pattern of burned areas based on the relatively short data record used here (~30 years) could signal not only GHG warming but the effects of natural variability, such as the Interdecadal Pacific Oscillation (IPO; Dong & Dai, 2015). Here, we focus more on the GHG warming effect, based on our previous modeling results. Modeling studies have suggested increased atmospheric dryness, that is, the reduction in relative humidity (RH) and the increased frequency and duration of dry spells in the subtropics and midlatitudes located over the western regions of major continents. These could be a component of a canonical global pattern of precipitation and large-scale circulation in response to GHG-induced warming (Lau et al., 2013). This pattern involves changes in the Hadley circulation (HC), linking a narrowing of the intertropical convergence zone (ITCZ) with enhanced precipitation, to an expanding subtropical subsiding zone with

reduced RH in the middle and lower troposphere via the so-called Deep Tropical Squeeze (DTS) radiation-dynamical feedback effect (Lau & Kim, 2015, 2017). The reduction in near-surface RH is important to the occurrence and spread of wildfires because of its close relationship to the water stress on vegetation. Low near-surface RH and high temperatures increase the vapor pressure deficit (VPD), enhance the evaporative demand, and accelerate the drying of vegetation, resulting in increased fire fuel and potential for large and severe wildfires (Holden et al., 2018; Seager et al., 2015; Williams et al., 2014). The physical relationships among wildfires in NA and regional feedback processes to changes in the large-scale circulation, global dryness, and linkages to GHG-induced warming are still poorly understood. In this paper, we aim to provide observational evidence revealing these relationships and shed new light on the underlying regional climate processes affecting wildfire trends in NA and linkages with climate change under GHG warming.

2.2 Data and methods

Data analyses are conducted using multiple independent datasets of wildfires and climate control variables. For wildfire data, we used the burned area information available from the MTBS database (Eidenshink et al., 2007) and Canadian National Fire Database (CNFDB). MTBS maps the burned area across all lands in the U.S from 1984 to present, including all fires 1000 acres or greater in the western U.S. and 500 acres or greater in the eastern U.S. Burned areas are mapped by using Landsat reflectance data to generate a Normalized Burn Ratio (NBR) for each pre-fire and post-fire target areas and then create a differenced Normalized Burn Ratio (dNBR). In our study, a total of 12,279 large wildfires were examined for U.S. from MTBS dataset.

Although large wildfires account for a small portion of total number of wildfire frequency, these large wildfires contribute to nearly 95% of total burned area. In addition, we use the Canadian National Fire Database (CNFDB) for the region of Canada. This collection of forest fire data is available from the Canadian fire management agencies. Unlike MTBS, NFDB dataset includes all sizes of forest fires. We selected wildfires with size larger than 500 acres to be consistent with MTBS. For NFDB, a total number of 13,614 large fires are examined.

For climate control variables, we used relative humidity (RH) from HadISDH global monthly land surface dataset (latest version 4.0.0.2017f) provided by the Meteorological Office Hadley Centre, which is derived from quality controlled sub-daily HadISDH stations since 1973. The RH data are monthly gridded at 5° by 5° resolution. Despite its relative coarse spatial resolution, it is a unique, in situ observations-only climate-data gridded product that is homogenized and physically consistent (Smith et al., 2011; Willett et al., 2014). Total cloud amount was obtained from the International Satellite Cloud Climatology Project (ISCCP). The new H-series of ISCCP extends the period of record to 1982-2014, providing monthly averages of cloud properties at 1° spatial resolutions (Rossow & Schiffer, 1991). Shortwave radiative fluxes data is available from Surface Radiation Budget (SRB) from NASA, which covers a 24 year (1984-2007) with 1º x 1º global grid derived from satellite-derived cloud parameters, reanalysis meteorology, and a few other ancillary data sets. For drought estimates, we used the Palmer Drought Severity Index (PDSI) from NCAR (Dai et al., 2004), which uses both temperature and precipitation data to estimate relative dryness PDSI. The monthly gridded air temperature (land) used are from

University of Delaware, this product uses a large number of station data, including the GHCN2 (Global Historical Climate Network), and complements the ICOADS (International Comprehensive Ocean-Atmosphere Data Set) dataset well. For large scale circulation analysis, we used five reanalysis products from MERRA2, NCEP2, ERA-Interim, JRA55, and 20CR respectively (Compo et al., 2011; Dee et al., 2011; Gelaro et al., 2017; Kanamitsu et al., 2002; Kobayashi et al., 2015) (See Table S2, for more detailed information for each dataset).

Table 2.1. Detailed information about the five reanalysis datasets.

Name	20CR	ERA-Interim	JRA55	MERRA2	NCEP2
Source	NOAA-CIRES	ECMWF	JMA	NASA	NCEP-NCAR
Atmospheric forecast system	Global Forecast System	Integrated Forecast System	Global spectral model	Goddard Earth Observing System	Global Forecast System
Data assimilation method	Three-dimensional variational data assimilation (3DVAR)	Four-dimensional variational data assimilation (4DVAR)	4DVAR	3DVAR	3DVAR
Satellite data processing	/	Fast Radiative Transfer Model	Fast Radiative Transfer Model	Community Radiative Transfer Model	Retrieved
Spatial resolution	2°×2°×24-levels	0.7°×0.7°×37-levels	1.25°×1.25°×37-levels	0.5°×0.625°×42-levels	2.5°×2.5°×17-levels
Time period	1851–2014	1979-present	1958-present	1980-present	1979-present
Reference	Compo et al. (2011)	Dee et al. (2011)	Kobayashi et al. (2015)	Gelaro et al. (2017)	Kanamitsu et al. (2002)

For fire datasets, we selected fires from May to September as fire season and fires are identified as wildfires (natural). All fires labeled as prescribed (man-make) fires were excluded. To facilitate quantitative analysis, we processed the above burned area data into 1° x 1° spatial grid data on monthly temporal resolution. Similarly, the original NFDB data were processed to 1° x 1° grid data as MTBS. Reanalysis datasets are remapped onto a uniform 2.5°×2.5° grid by using bilinear interpolation to calculate the multi-reanalysis ensemble (MRE) mean.

First, analysis was conducted for wildfire datasets for the entire North America, to identify regions with pronounced regional trends in wildfires and surface air temperature. Second, trend patterns of key climate control variables of surface relative humidity, cloudiness, net downward surface solar radiation, and drought severity were constructed and examined for correlations with wildfire trends for each sub-regions of WUS, AK and WCC respectively. Third, circulation and precipitation features associated with global warming trends over the North Pacific and North America, as well as vertical profiles of temperature, RH and vertical motions are examined over each sub-regions of WUS, AK and WCC using ensemble mean of five re-analysis products. Trends for all variables including fire records and climate variables are based on linear regression as default. The correlation between burned area and various climate variables used Pearson correlation. Student-t test was used to assess the significance (p-values) of monotonic trends in fire and climate variables.

2.3 Results

2.3.1 Wildfires trends over North America

To begin, we examine the time variations and trends of large fire burned area, and surface air temperature averaged over North American (NA), and separately for US and Canada. The NA time series of burnt area (Figure 2.1a) shows large interannual variability, and a strong positive trend during 1984-2014. The positive trend of burned area over NA is statistically significant ($p < 0.05$), as found in previous studies (Dennison et al., 2014; Picotte et al., 2016). The average of total burned area in 2010s is more than double the mean during 1980s. Separating into US and Canada regions, the increasing wildfires trend is mainly contributed by US, while Canada shows considerable variability but no significant long-term trend. On the other hand, area-averaged surface temperature (Figure 2.1b) shows similar warming trend (+ 0.3 ^{o}C decade^{-1}) and variability for both US and Canada. In contrast to the trends in wildfire burnt area, the NA warming appears to be driven more by the warming of Canada than the US. Hence, on a continental scale, a warmer temperature appears to be a necessary but not sufficient condition for increased wildfires over North America. To understand the differences between the warming and wildfires trends in US and Canada, we need to examine the spatial distribution of wildfires, and their relationships with the regional and global climate forcing and feedback.

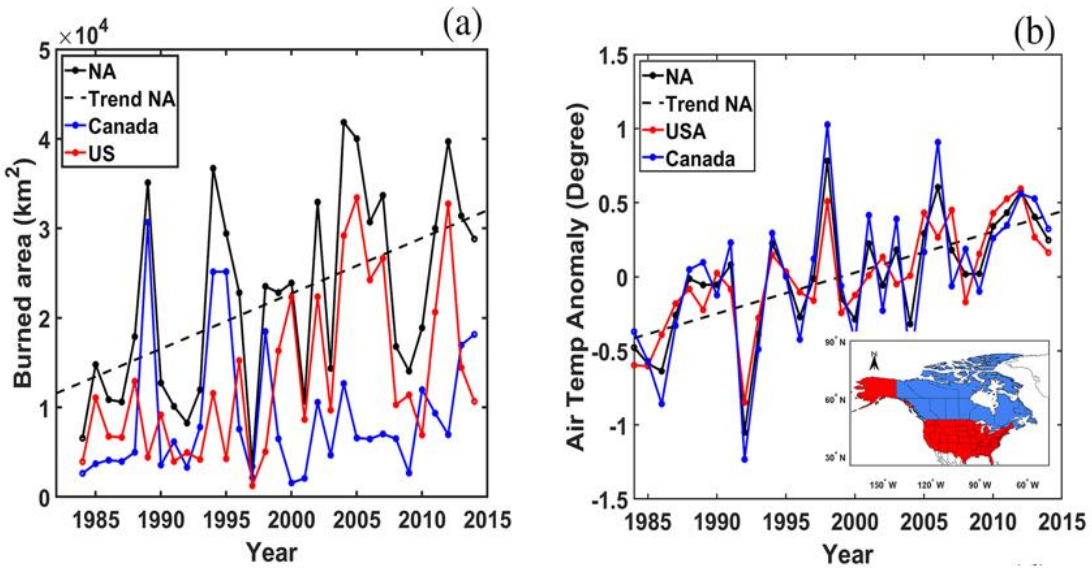

Figure 2.1 Wildfire and warming trends in North America from 1984–2014 (May to September). Time series of (a) burned area (unit: 10^4 km^2) and (b) surface air temperature anomalies (^oC) in North America (black curve), the US (red curve), and Canada (blue curve)

The spatial pattern of large fire burned area trend over NA during 1984-2014 (Figure 2.2a) is highly asymmetric in the sense that while both negative and positive trends are present, significant signals ($p<0.05$) are found clustered only in regions with positive trends. No significant clusters of negative trends are found. Three regions of strongly increasing burnt areas (> 50-100 km^2 $decade^{-1}$) stand out: western US (WUS), Alaska (AK), and Western-Central Canada (WCC). WUS includes states of Washington, Oregon, northern California, Idaho, and mountain regions of Arizona and New Mexico. WCC includes the provinces of Alberta, Saskatchewan and southern Northwest Territories. Negative but weaker trends ($p>0.05$) in burned area are found over the center and west of Northwest Territories, Manitoba and part of Quebec province. Over WUS, the burnt area shows a robust, steady long-term trend (total area of 3350 km^2

decade^{-1}) with strong interannual variability (Figure 2.2b). In contrast, for AK and WCC, trend signals are much weaker, and appear to be affected by episodic occurrences of a few exceptionally large fires (Figure 2.2c, d). The asymmetry and highly regional distributed trend pattern in burnt areas, as well as different temporal variability among WUS, AK and WCC suggest the effect of a large-scale steady background forcing, i.e., overall warming of North America (Figure 2.3), modulated by regional scale climate feedback processes.

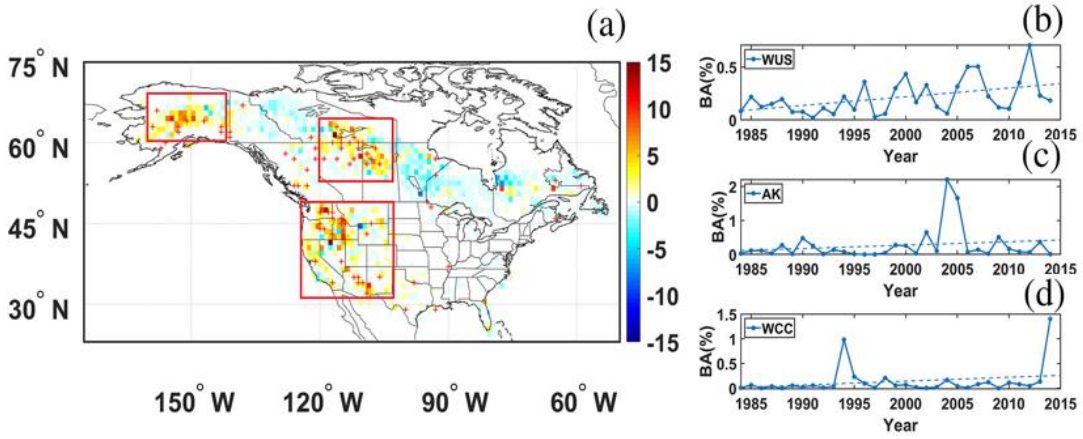

Figure 2.2 (a) Spatial pattern of linear trends in burned area per 1° × 1° grid box (unit: km^2 decade^{-1}). Statistically significant trends ($p < 0.05$) are denoted by red crosses. (b-d) Time series of burned area percentages with trend lines averaged over domains outlined by the red rectangles in (a), representing (b) the western US, (c) Alaska, and (d) western central Canada.

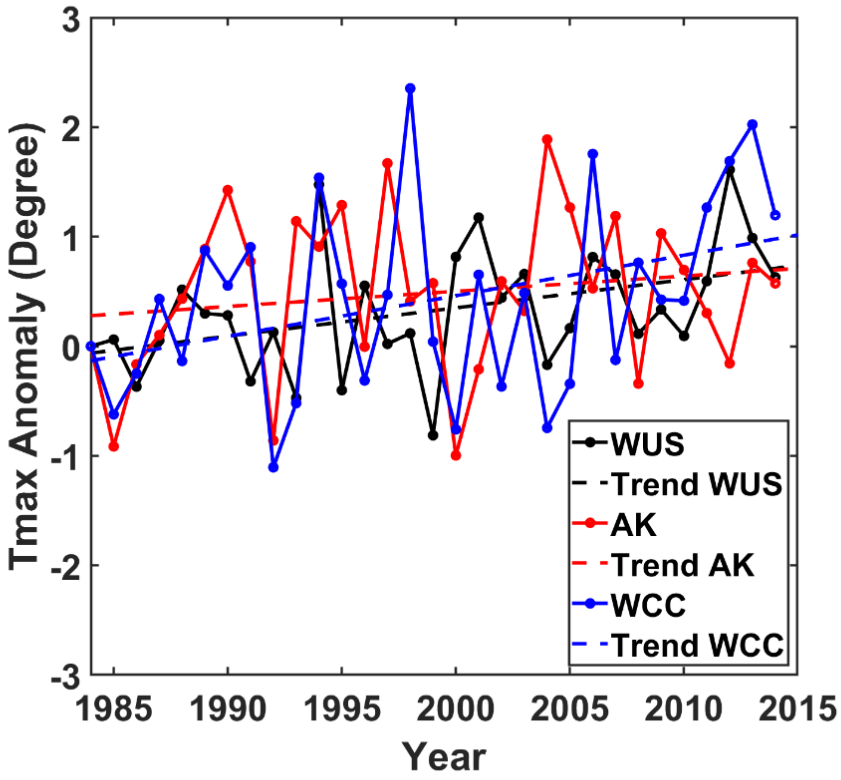

Figure 2.3 Time series of maximum air temperature anomalies (unit: ^{o}C) in the western US (WUS, black), Alaska (AK, red), and western-central Canada (WCC, blue) from May-September of 1984-2014. The linear trends are shown as dashed lines. Data is from the Climatic Research Unit Timeseries V4.04.

2.3.2 Related trends in key climate control variables

As discussed previously, a reduction in RH will likely lead to increased surface VPD resulting in accelerated drying of the vegetation, and increased potential for wildfires (Holden et al., 2018; Williams et al., 2014). Furthermore, an RH deficit is also likely associated with suppressed clouds and precipitation. Less clouds will lead to reduced SW cloud shielding, enhanced incoming surface SW radiation, leading to warmer land

and increased evapotranspiration, and hence faster, and sustained warming and drying of the atmosphere-vegetation system, with more raging wildfires. For convenience, we refer to this chain of processes as the regional climate feedback exacerbating wildfires (RCFW). In the following, we examine the validity of RCFM in affecting the long-term trends in wildfires over NA, by conducting trend and correlation analyses on wildfires burnt areas with respect to several key climate control variables, i.e., surface RH, cloud amount, shortwave downward radiation (SWDR) and PDSI. The trend patterns of these climate observables for the wildfire season (May-September) are shown in Figure 2.4. Overall, a north-south dipole pattern in reduced surface RH is found over North America, with strong negative trends (2-3% decade^{-1}) over the southern and western US, and positive trends over northern Midwest and central Canada (Figure 2.4a). Over Alaska, the RH trend signal is mixed. Total cloud cover (Figure 2.4b) shows reduction in broad swath spanning Alaska, Northwest territories the US Midwest and Eastern US, with the maximum reduction (10-15% decade^{-1}) over the WUS. The overall reduction in cloudiness is comparable to previous studies which showed overall reduction in cloudiness up to 5% decade-1 for contiguous US over a similar period (Free et al., 2016; Sun et al., 2015). Increased SWDR is found over the WUS, coinciding with the regions of strong reduction of clouds and reduced surface RH (Figure 2.4c). Over northwestern Canada, SWDR trends negative, except in southern Alaska, just north the Gulf of Alaska, where the trend is weakly positive. The strong positive SWDR trend over WUS is consistent with the 'global brightening' since mid-1980 (Wild, 2011), attributable in part to reduced cloudiness and aerosols. From

PDSI (Figure 2.4d), a large part of the southern and WUS, central Canada and part of southern Alaska are experiencing increasing drought conditions (negative PDSI).

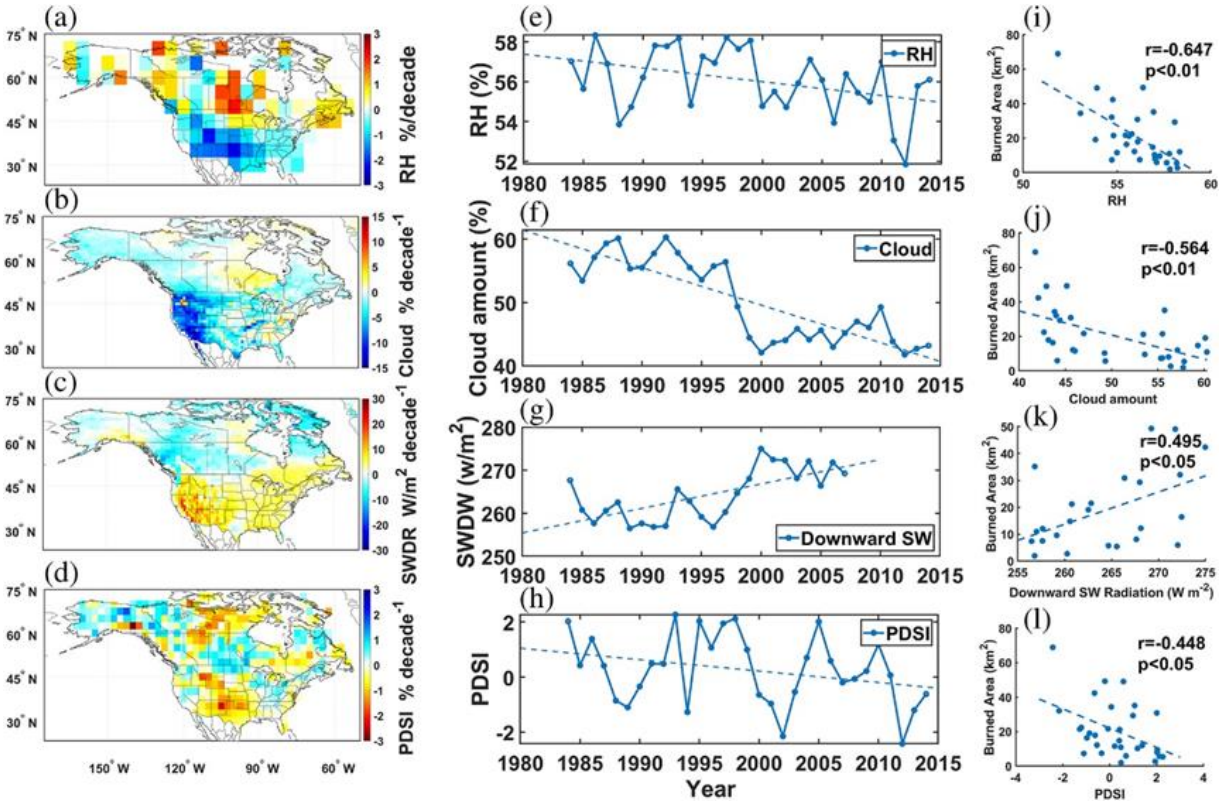

Figure 2.4 Observed climate changes during 1984–2014 (May-September). Spatial linear trend patterns of (a) near-surface RH (unit: % decade^{-1}), (b) cloud cover (unit: % decade^{-1}), (c) downward SW radiation (W m^{-2} decade^{-1}), and (d) PDSI over North America. Time series of (e) near-surface RH (unit: %), (f) cloud cover (unit: %), (g) surface downward SW radiation (unit: W m^{-2}), and (h) PDSI averaged over the western US. Panels (i) to (l) show burned area as a function of RH, cloud amount, downward SW radiation, and PDSI, respectively.

Based on the above results, we select for further analyses the areal mean serial correlations of burnt areas to RH, cloud amount, SWDR and PDSI respectively for three key regions of WUS, AK and WCC that show strong positive trends in large wildfires burned areas (See Figure 2.1c). During the last three decades, WUS has

experienced decreasing RH (~ 0.7% decade^{-1}, Figure2.3e), decreasing cloud amount (5.9% decade^{-1}, Figure 2.4f), increasing SWDR (~5.7 W/m^2 decade-^{1}) reached the land surface (Figure 2.4g), and increasing drought severity (negative trend of 0.4% decade^{-1} in PDSI, Figure 2.4h). Worth noting is that all the aforementioned climate observables show considerable interannual and interdecadal variabilities, linked to natural modes of climate variability, such as the El Niño-Southern Oscillation, the Pacific Decadal Oscillation (similar to IPO), and the Atlantic Multi-decadal Oscillation that could influence fire weather, fuel availability, and ignition (Kitzberger et al., 2007; Pan et al., 2018; Schoennagel et al., 2005; Wang et al., 2014). Considering both trends and natural variability, the strongest correlations with burned area are, in descending order, reduced RH (-0.65, $p < 0.01$), cloud amount (-0.56, $p < 0.01$), SWDR ($+0.49$, $p < 0.05$), and PDSI (-0.45, $p < 0.05$), supporting RCFW (Figures 2.4i–l). Note that our study period overlaps with a phase change in IPO (Figure 2.5), switching from a warm phase (1984–1998) to a cold phase (1999–2014). This IPO phase change likely weakened the "underlying" warming trend during our study period (Dong & Dai, 2015). An additional analysis of the co-variability of the IPO index with RH (detrended) showed mostly weak and insignificant negative correlations (correlation coefficient, $r < 0.3$, $p > 0.05$) over much of NA (see Figure 2.6). This implies that the surface humidity deficit trend was likely weakened by the negative phase of the IPO during the latter portion of the study period. Examination of the IPO-burned area correlation pattern (Figure S4) shows positive correlations most pronounced over AK, WCC, and the Pacific Northwest. Given the dominance of the cold phase of the IPO during 1999–2014, these positive correlations imply reductions in burned areas, contrary to the underlying

increasing trend in burned areas in these regions. This may explain, in part, why the positive trends in burned area are much less pronounced in AK and WCC compared to the WUS (Figures 2d and 2c). In short, the IPO likely confounds the GHG warming signal as represented by the linear trend pattern in our analysis regionally.

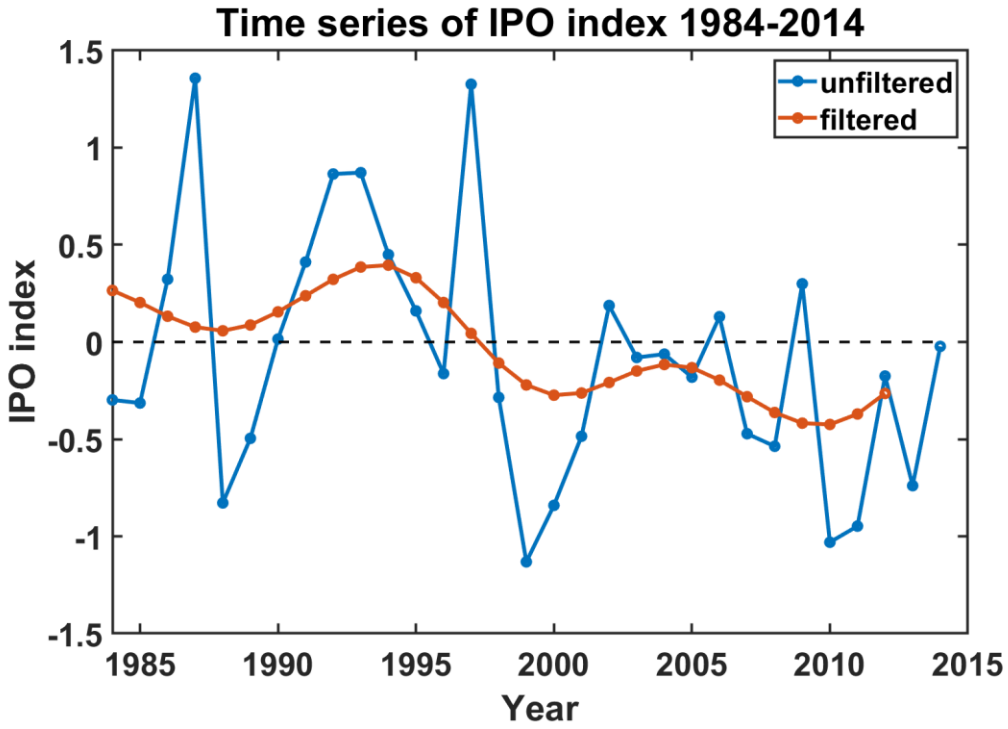

Figure 2.5. Filtered (orange) and unfiltered (blue) time series of the Interdecadal Pacific Oscillation (IPO) index from May-September of 1984-2014. Monthly IPO index data are obtained from HADISST(https://psl.noaa.gov/data/timeseries/IPOTPI/).

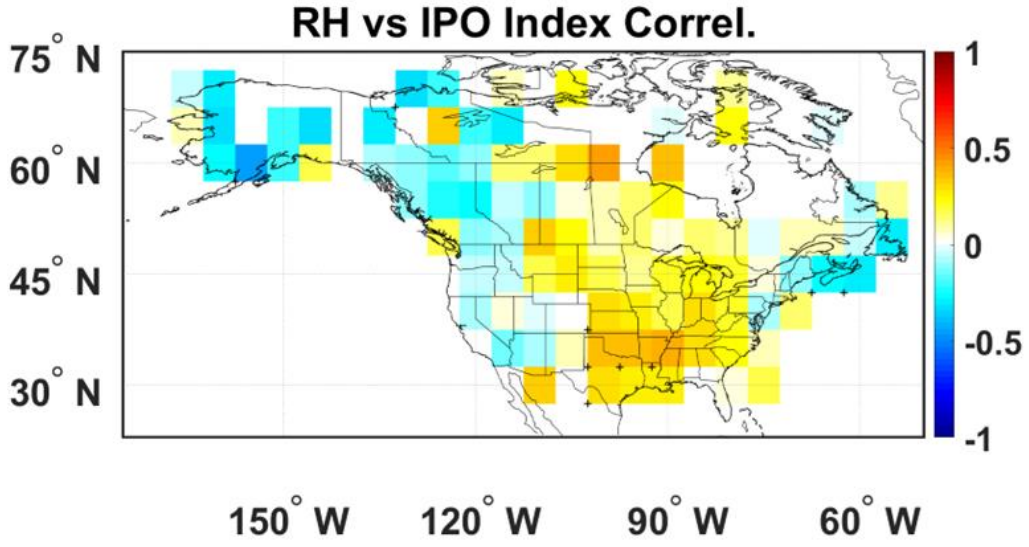

Figure 2.6. Spatial pattern of correlations between near-surface relative humidity (RH) and the Interdecadal Pacific Oscillation (IPO) index from May-September of 1984–2014. Statistically significant ($p < 0.05$) trends are denoted by black crosses.

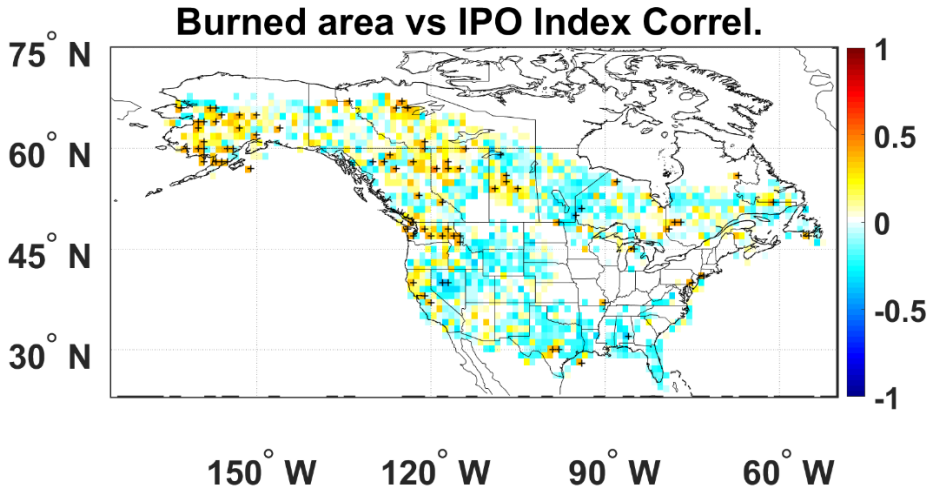

Figure 2.7 Same as Figure 2.6 except for correlations between burned area and the Interdecadal Pacific Oscillation (IPO) index. Crosses indicate areas with confidence level exceeding 10%.

Correlation analyses were carried out for AK and WCC similar to WUS, and results for all three regions are summarized in Table 2.2. Robust trends of burnt areas and significant correlations with all four climate observables are found only in WUS. For AK, no significant correlations are found in any of the climate observables. For WCC, significant relationships ($p<0.05$) are found only in RH and PDSI. These suggest that RCFW works for WUS only, but not AK and WCC. The reasons for the regional differences are explored in the next section.

Table 2.2. Slopes of the linear regression lines for the near-surface relative humidity (RH), cloud cover, surface downward shortwave (SW) radiation, and the Palmer drought severity index (PDSI), and correlations with burned area over the western US (WUS), Alaska (AK), and western-central Canada (WCC) from May-September of 1984–2014. The first column for each variable denotes the slope of the time series trend (in unit per decade). The second column denotes the correlation with burned area. Values marked with ** (*) represent $p < 0.01$ ($p < 0.05$).

Region	Burned Area	RH		Cloud Cover		Downward SW		PDSI	
	slope km^2/decade	slope %/decade	Corr	slope %/decade	Corr	slope W/m^2/decade	Corr	Slope $decade^{-1}$	Corr
WUS	7.5**	-0.69*	-0.64**	-5.9**	-0.56**	5.7**	0.49**	-0.4*	-0.44*
AK	8.6**	0.2	-0.002	-0.97	-0.03	3.2	-0.05	0.4	-0.23
WCC	3.9*	-0.4	-0.4*	0.02	0.25	-5.2*	-0.01	-0.5*	-0.43*

2.3.3 Wildfires and Greenhouse Warming

Previous observational and modeling studies have identified features in the large-scale circulation that are likely attributable to greenhouse warming. These include among others, multi-decadal trends in a strong warming and moistening of the tropical

atmosphere(Q. Fu et al., 2011; William K.-M. Lau et al., 2013; B. D. Santer et al., 2008; Benjamin D. Santer et al., 2016); a rise of the tropical tropopause(Lorenz & DeWeaver, 2007; Seidel & Randel, 2007); a widening of the subtropics and poleward migration of midlatitude storm tracks(Feng & Fu, 2013; Hu & Fu, 2007; Lu et al., 2007; Seidel et al., 2008; Yin, 2005), and expansion of the global dry lands(Dai, 2011; Huang et al., 2016). More recently, our CMIP5 model results have demonstrated that the aforementioned changes are underpinned by the "Deep Tropical Squeeze" (DTS) i.e., a structural change in the Hadley Circulation (HC) under greenhouse warming, featuring a narrowing ITCZ core with increased precipitation, linked to increased subsidence and reduced RH in the subtropics and midlatitudes (R. Fu, 2015; W. K. M. Lau & Kim, 2015).

In the following, we examine the changes in the large-scale circulation affecting the northeastern Pacific and North America climate using re-analyses data, in order to shed new light on the possible relationship between wildfires in North America and greenhouse warming. To increase the robustness of the results, we have computed the long-term trend patterns of tropospheric temperature, RH, sea level pressure, winds, vertical motion, and precipitation for 1984-2014, based on the ensemble mean of 5 independent re-analyses datasets i.e., MERRA2, ERA-Interim, NCEP2, JRA55 and 20CR (see Table 2.1for detailed description of each dataset)

As revealed in the latitude-height cross-section of zonal annual mean temperature trend pattern (Figure 2.8a), during 1984-2014, there has been strong warming of the entire troposphere and cooling in the lower stratosphere (above 150 hPa) - a well-recognized signature of global greenhouse warming (Q. Fu et al., 2011; B. D. Santer et

al., 2008; Benjamin D. Santer et al., 2016). Associated with the tropospheric warming, the RH trend (Figure 2.8b) displays a characteristic pattern indicating increased RH in the deep tropics, but strong RH reduction in the tropical upper troposphere, and descending arms of regions of RH deficit in the tropospheric column to the earth surface in the subtropics and midlatitudes of both hemispheres. The RH trend pattern is similar to model projections attributable to global warming (Sherwood et al., 2010). The pattern can be understood in terms of the faster rate of increased saturated vapor pressure with temperature as governed by the Clausius-Clapeyron law of thermodynamics, compared to the actual increase in ambient vapor pressure due to transport processes (W. K. M. Lau & Kim, 2015; Sherwood et al., 2010). Increased dry advection from above by enhanced anomalous descent in the subtropics and mid-latitudes due to the expansion of the HC under greenhouse warming can lead to further RH deficit in the lower troposphere and near surface over these regions (Hu & Fu, 2007; W. K. M. Lau & Kim, 2015). In association with the trend in reduced zonal mean RH, an east-west dipole anomalous sea-level pressure (SLP) pattern, with high SLP centers over the North and East Pacific and WUS coupled to low SLP centers over the rest of North America is established during the peak wildfires season (May-September), signaling an intensification and expansion of the North Pacific Subtropical High (NPSH, Figure 2.8c). The eastward extension of the NPSH, signaled by the development of an anomalous high SLP center over WUS, is likely to be strongly affected by regional topographic effects. Specifically, an anomalous anticyclonic circulation center is found anchored over the elevated arid region of the Great Basin east of the Rocky Mountains (Figure 2.8c). As the cold, dry air masses descend in a

clockwise rotation from high elevations into lower valley regions of the coastal mountain ranges they are heated by adiabatic compression, causing a further rapid drop in relative humidity, and gusty winds due to air density differences. These hot and dry offshore winds combined with dry vegetation during summer and fall, would fan more large wildfires. The anomalous SLP center will likely intensify the Santa Ana and Diablo winds (in the fall season), affecting wildfires and prolonging the fire season. Wind gusts affecting wildfires, and relationships with greenhouse warming are currently subjects of numerous studies and debate (Guzman‐Morales & Gershunov, 2019; Hughes et al., 2011; Jin et al., 2015; Miller & Schlegel, 2006; Yue et al., 2014).

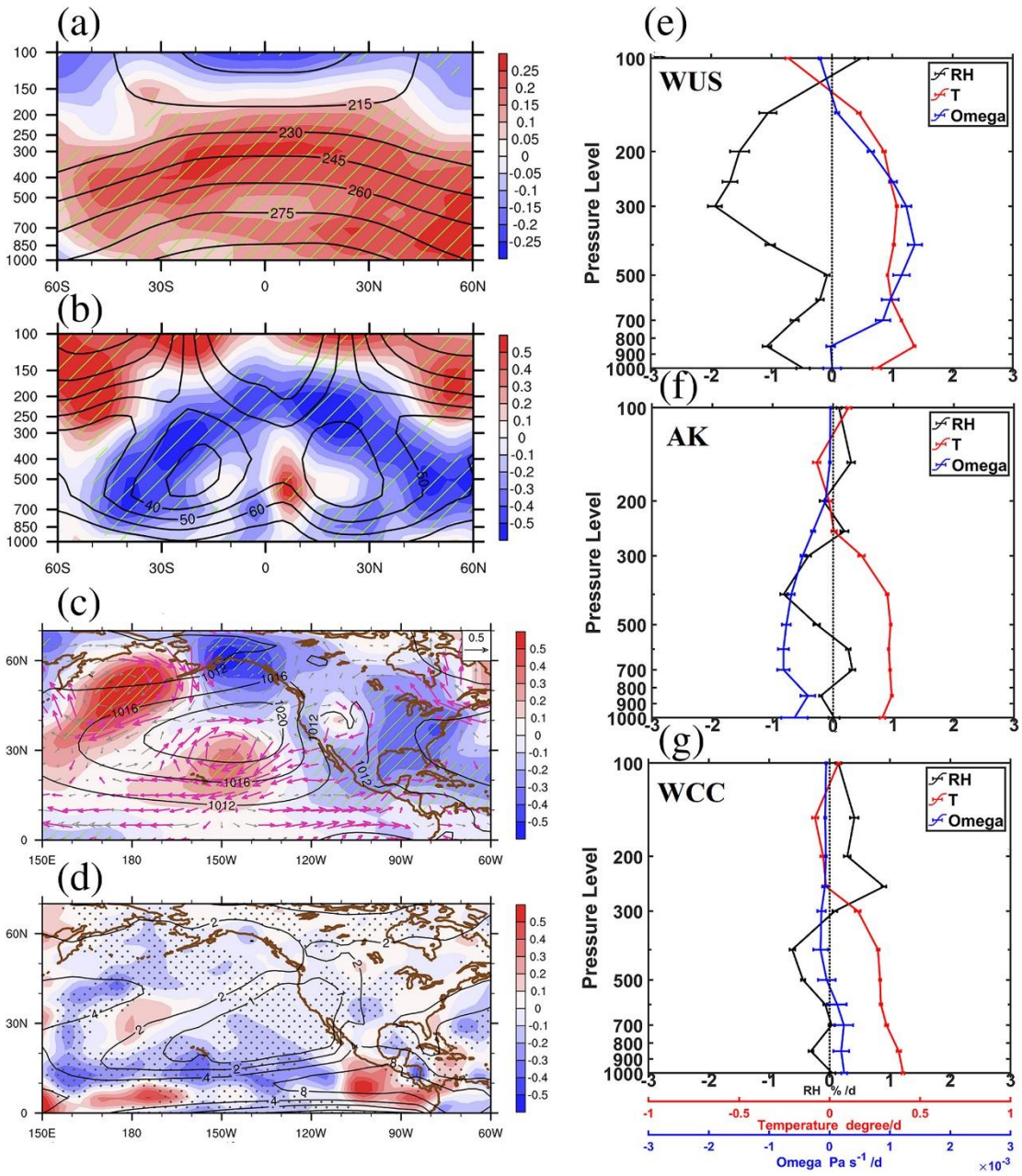

Figure 2.8 Left panels: Latitude-height cross-sections of the linear trends (1984–2014, annual mean) in (a) temperature (unit: °C decade^{-1}) and (b) RH (unit: % per decade^{-1}). Spatial patterns of mean linear trends (1984–2014, May-September) in (c) sea-level pressure (unit: hPa decade^{-1}) and 700-hPa winds (arrows, m s^{-1} decade^{-1}), and (d) precipitation (mm day^{-1} decade^{-1}) and 500-hPa vertical motion (Pa s^{-1} decade^{-1}). Trends are shown by color shading, and the contours are the 1984–2014 climatology. Areas

with anomalous descending motions are indicated by black dots in (d). Right Panels: Vertical profiles of the linear trend (1984–2014, May-September) in temperature (red curve, °C decade^{-1}), RH (black curve, % decade^{-1}), and vertical p-velocity (blue curve, Pa s^{-1} decade^{-1}), with positive values denoting sinking motion for (e) the western US, (f) Alaska, and (g) western-central Canada, based on the ensemble mean of five reanalysis datasets. Standard errors of the mean are shown as horizontal error bars.

Strong trends in suppressed precipitation, and widespread anomalous sinking motion at 500 hPa are found over much of the subtropical and mid-latitude regions of Northeast Pacific and North America (Figure 2.8d). Analysis of time series of vertical motion at 500 hPa over the climatological NPSH region (30–45oN, 140–90oW) and burned area over WUS (Figure 2.9) shows significant correlation (r = 0.45, p value = 0.011), indicating a close relationship between WUS wildfire and enhanced subsidence in the descending branch of the HC. Also found is a strong reduction in precipitation in the northern edge of the ITCZ near 10-15^{o}N, and increased precipitation near the equator. The aforementioned features mirror those associated with the DTS, under global warming (W. K. M. Lau & Kim, 2015). Note that the WUS is geographically located at the semi-arid zone at the eastern edge of the North Pacific Subtropical High. Hence it is possible that changes in the RH, cloudiness, SWDR, precipitation, and circulation arising tropical influence due to global warming may affect wildfires in WUS region more strongly compared to other regions in North America. This may explain, in part, the lack of strong and coherent signals in burnt area to our chosen climate control variables, in the other two regions with significant burnt area trends, i.e., AK and WCC. In these two regions, influence from other factors such as storm track and jet stream dynamics, as well as increased lightning ignitions and northward expansion of the

boreal forest associated with Arctic warming may play more important roles (Box et al., 2019; Veraverbeke et al., 2017a).

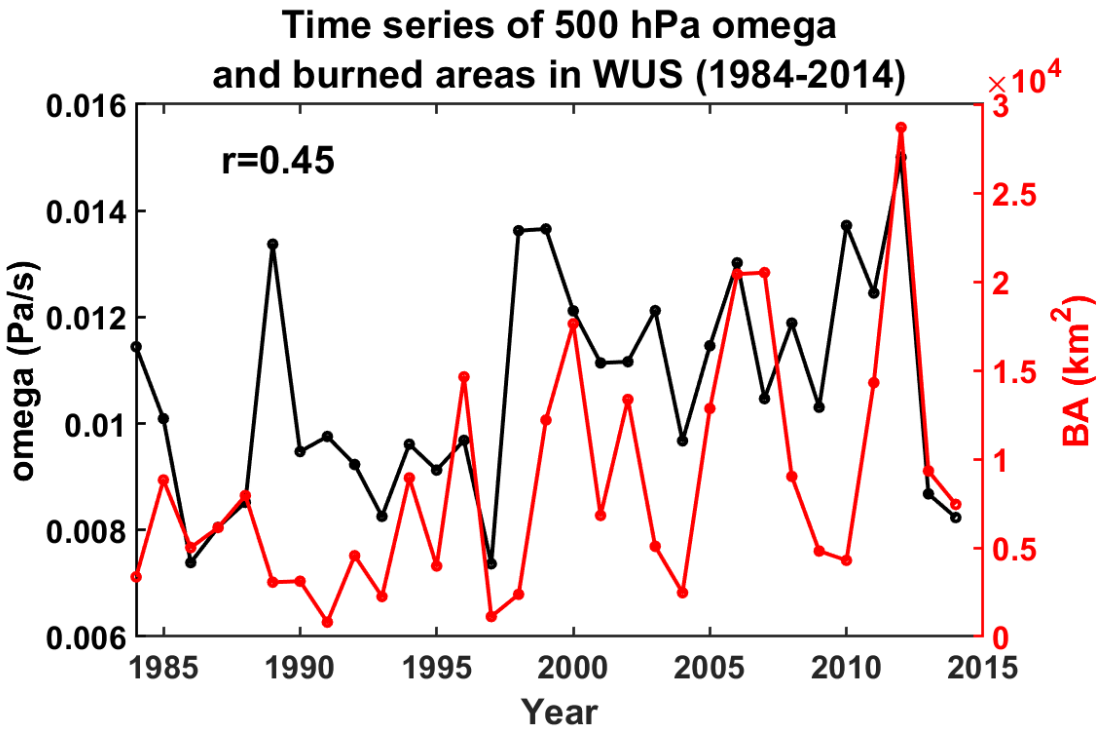

Figure 2.9. Time series of the mean omega at 500 hPa (black) over the descending branch of the HC over the subtropical North Pacific (90-140°W, 30-45°N) and burned areas (red) in WUS from May-September. Positive value of omega denotes descending motion. Serial correlation of the time series, r =0.45, with p-value= 0.011.

To further explore RCFW over WUS, we examine the trend patterns in vertical profiles of RH, vertical p-velocity (omega) and temperature from the multi-reanalysis data averaged over WUS (Figure 2.8e) during the wildfire season (May-September). Most noteworthy is the robust warming trend (0.3-0.5 C decade^{-1}) of the atmospheric column from surface to above 200 hPa. A strong trend in sinking motion (positive omega) is found from 800hPa to 150hPa with a maximum rate of up to 1.5 10^{-3} Pa/s

decade^{-1} near 400 hPa. As discussed previously, both increased temperature and subsidence can lead to a large RH deficit. The RH profile shows reduction over the entire atmospheric column, with maxima decreasing trend about 2% decade-1 at the 300hPa, and a secondary maximum (1% decade^{-1}) near 850 -900 hPa. This secondary low-level maximum RH reduction is likely related to the dry advection effect of the enhanced offshore low-level flow, as well as increased intensity of warmer and drier winds by adiabatic compression, descending from higher elevation inland to coastal areas across the central and southern WUS region (See discussion for Figure 2.8c). As shown previously (see Figure 2.4), the RH deficit is associated with reduced cloud and precipitation and increased surface solar radiation that is likely to enhance the warming of the earth surface. Additionally, adiabatic warming of the descending air would further amplify the warming of the atmospheric column, further reducing RH. These feedback processes would thus amplify the greenhouse warming and drying of atmosphere-land. At the same time, reduced RH leads to increased VPD, enhanced evapotranspiration from leaves and thus accelerates the drying of the vegetation and land, promoting more wildfires. Over AK and WCC (Figure 2.8f-g), while the tropospheric warming signal is strong, RH and vertical motion do not show coherent signals in the vertical, indicating a lack of RCFW.

2.4 Conclusion

A comprehensive analysis of long-term wildfire datasets in North America revealed the most significant increasing trend in Western US, even though temperature rise is more pronounced in high latitudes. A plausible mechanism is put forth, involving regional climate feedback on wildfire as follows. A RH deficit associated with drying

of the subtropics under global warming inhibits convection, suppresses cloudiness and precipitation, and minimizes the shortwave cloud shielding effect, resulting in enhanced net downward surface shortwave radiation. The increased shortwave radiation accentuates an already warming land-atmosphere system, and through RCFW amplifies the RH deficit, increasing the VPD and drying of vegetation, and potentially spurring more severe wildfires. The response over western US is likely a regional manifestation of a global drying trends associated with the expansion of the subsidence branch of the Hadley Circulation (HC), coupled to increased precipitation of the ITCZ in the deep tropics, that have been attributed to greenhouse warming in previous studies (Hu & Fu, 2007; W. K. M. Lau & Kim, 2015). Our results also show that the development of an anomalous surface pressure center over the Great Basin in associated with global drying trend and HC changes, may be instrumental in enhancing offshore winds, fanning more large wildfires over the WUS.

The Western US, being geographically located over the semi-arid zone at the eastern edge of the North Pacific Subtropical High, is more likely subjected to the strong influence from circulation changes and regional feedback processes, exacerbated by tropical warming and subtropical drying. Over Alaska, and Western Central Canada, the other two regions in North America with significant, but weaker long-term trends in large wildfire burnt areas, RCFW is found to be weak or absent. We suggest this may be due to the high-latitude locations of these regions, where tropical influences, such as DTS, on wildfires are diminished. The wildfires burnt areas in these regions may be more impacted by additional climate controls such as storm track and jet stream dynamics, as well as possibly increased lightning ignition, and northward migration of

the boreal forest associated with Arctic warming (Box et al., 2019; Veraverbeke et al., 2017b). Finally, it remains to be investigated RCFW is operative over other continental vegetated land regions (Asia, Europe, South Africa, Australia, and South America) affected by global warming and atmospheric drying. If so, more wildfires on a global scale is likely to increase emissions of greenhouse gases, and light-absorbing aerosols such as black carbon and organic carbon exacerbating global warming, thus completing the climate-wildfire feedback loop (William Ka-Ming Lau & Kim, 2017; Liu et al., 2010, 2014). These are important subjects of future studies.

Chapter 3: An assessment of climate and weather extremes driving the western U.S extraordinary wildfire in 2020

3.1 Introduction

The 2020 wildfire season in the western United States was one of the most devastating on record. Large portions of California, Oregon, and Washington State were affected, with fires burning through millions of acres of land, destroying homes, and claiming lives. In California, the August Complex Fire became the largest wildfire in the state's history, burning more than one million acres. Oregon was also hit hard, with the Beachie Creek Fire and the Lionshead Fire burning through more than 500,000 acres of land. The 2020 fire season in the western U.S. had a significant and far-reaching impact on human society; over ten thousand of structures have been damaged or destroyed, over 30 lives have been lost, thousands of people forced to evacuate their homes, and many areas experienced hazardous or unhealthy air conditions for weeks.

These significant impacts may raise the doubt: what made the 2020 fire season in the western U.S. so exceptional? In fact, 2020 was one of the hottest years on record globally. The average global temperature in 2020 was about 1.02°C above the 20th-century average. This made 2020 the second-warmest year on record, just behind 2016 since 1880. This extreme hot condition also contributes significant wildfires that occurred other regions around the world, including in Australia and parts of South America and Siberia. Such high temperature would increase the vapor pressure deficit (VPD), thus increasing fire risk by drying fuels. Recent studies have suggested that 2020's widespread wildfire was clearly enabled by record-setting atmospheric dry

condition across much of western U.S, reflected by VPD (Higuera et al. 2020). Several studies focus on the 2020 fires in historical context in California, pointing out the extraordinary drought is the prominent factor (Keeley et al. 2021; Safford et al. 2022). 2020 Labor Day fires in Oregon were attributed to a series of factors including compound extremes of fuel dryness and low-level wind speed (Abatzoglou et al. 2021). However, detailed analysis of the exceptional 2020 fire season over WUS is still lacking, and the role of climate factors has not been fully explored yet. Thus, this study aims to provide a comprehensive assessment and understanding of the surface and atmospheric conditions associated with this extraordinary 2020 fire season by using satellite fire observations and ERA-5 reanalysis data.

3.2 Data and method

Wildfire data were obtained from two main sources: MODIS (moderate resolution imaging spectroradiometer) and MTBS (Monitoring Trends in Burn Severity). For MODIS, we choose the burned area product MCD64A1. This product consists of monthly, global gridded fire data with 500 m resolution from 2001 to 2020 (Gelaro et al. 2017). The MTBS dataset has been introduced in detail in Chapter 2.

For climate and weather parameters were obtained from the European Centre of Medium-range Weather Forecast ERA-5 reanalysis dataset. All data were processed at a 0.25° × 0.25° spatial resolution from 1980 to 2020. They include VPD, temperature, relative humidity (RH), precipitation, geopotential height, specific humidity and vertical velocity at several levels of the atmosphere.

In our study, we also analyzed dry lightning in the western U.S using the National Lightning Detection Network (NLDN) dataset. This dataset provides the daily cloud-

to-ground (CG) lightning totals from 1987-2020 and were processed to 0.25° × 0.25° grid to match the ERA-5 data. We defined dry lightning using a threshold of less than 0.25 mm of daily-accumulated precipitation provided by ERA-5 daily precipitation data. Note that this approach has its shortcomings including the unknown timing or duration of precipitation relative to lightning (Rorig and Ferguson 1999).

The study region focuses on the western U.S, which comprises a diverse and geographically extensive region of the country (Fig.3.1). In our study, we included states of California, Nevada, Arizona, Utah, Colorado, Wyoming, Idaho, Oregon, Washington, Montana, and New Mexico.

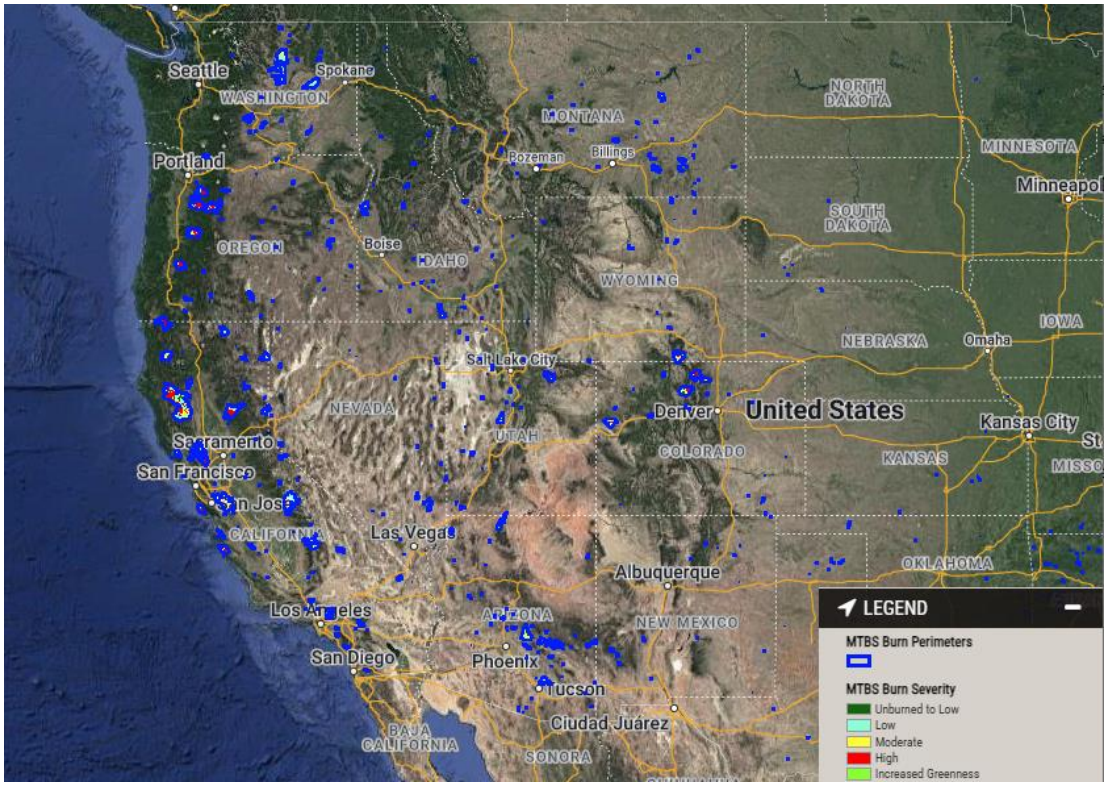

Figure 3.1 Study region of western U.S and MTBS burn perimeters in 2020.

3.3 Result

3.3.1 Burned area anomaly in 2020 in the WUS

Figure 3.2 shows the annual change of burned area in western U.S and each state from 1984 to 2021 (derived from MTBS product). 2020 stands out as a year of unprecedented wildfire activity in terms of the total burned (nearly 4×10^4 km^2), in particularly California (CA), Oregon (OR), and Colorado (CO) three states contributed to this record-breaking annual burned area anomaly in 2020.

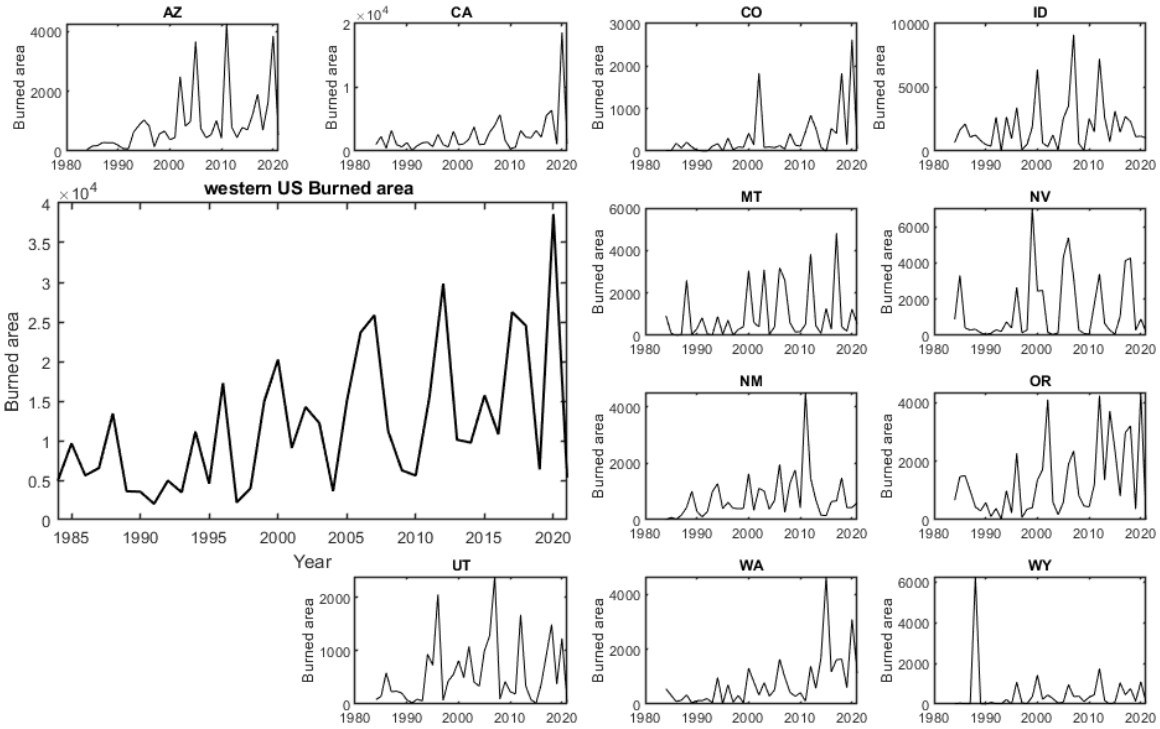

Figure 3.2 Annual variation of burned area in fire season for western U.S and for each state during 1984-2021.

The peak fire season in the western US typically occurs during the summer and early fall months, typically from late June to October (shown in Figure 3.3), when hot and dry weather conditions are most common. Southwest states including Arizona and New

Mexico have earlier wildfire peak season in June compared to other states (mostly in July or August). During this time, vegetation in many parts of the western US is dry and susceptible to human or lightning ignition, which can lead to the rapid spread of wildfires. From Figure 3.3, the western U.S. in August and Septermber of 2020 experienced much higher levels of wildfire activity than climatology. Over 1.8×10^4 km^2 area was burned during August and over 1.0×10^4 km^2 burned during September. It is noteworthy that total burned area in September is almost five times than the climatlogical value. The BA anomaly in August mainly comes from states of California, Colorado, Oregon and Utah, while in September the extreme anomaly are mostly from Northwest states including Oregon, Washington, Wyomin and Montana.

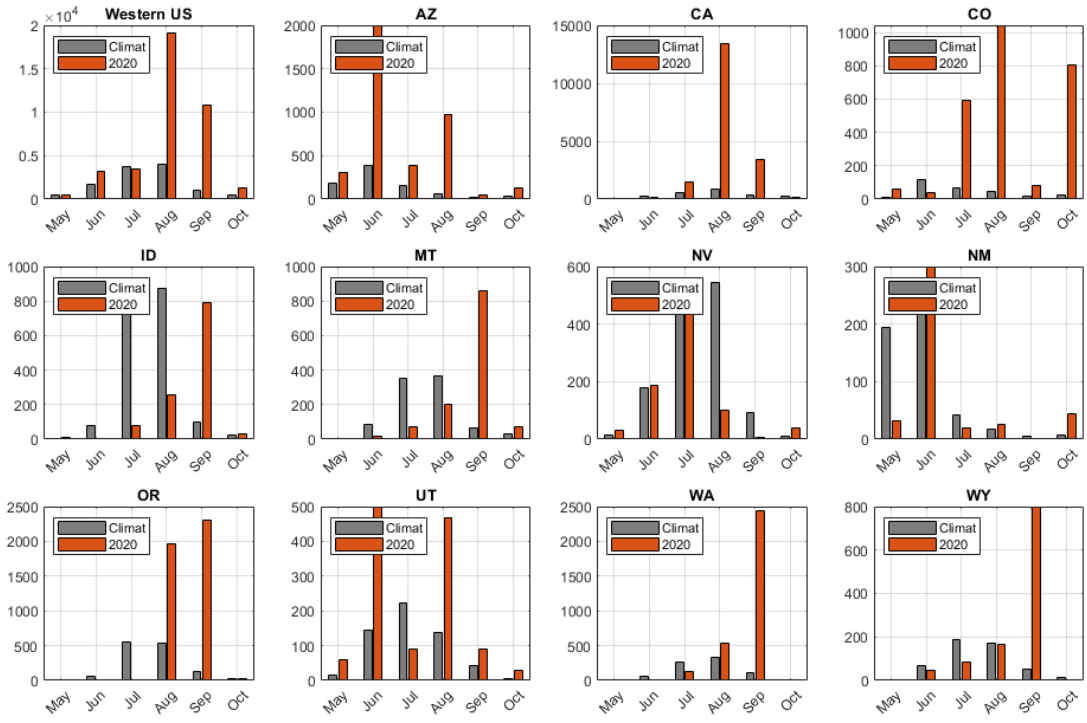

Figure 3.3 Monthly change (May to October) of burned area in 2020 compared to the climatology for western U.S and each state.

3.3.2 Climate factors associated with burned area trend

The major climatic drivers of recent increase in western US wildfire are mostly related to increased air temperature, higher VPD and decreased precipitation (Holden et.al 2018). Here we examined how the temperature, VPD and precipitation in 2020 fire season compared to the historical level since 1980 based on the ERA-5 reanalysis datasets. Figure 3.4 shows evidence that all three factors in western U.S have emerged outside of the range of historical experience in 2020. Temperature and VPD have emerged above 1σ natural variability level since 2017, and in 2020 August, they were above +2σ compared to the historical mean. For September, only VPD exceeded the 2σ threshold. All three climatic factors are closely related to the dangerous fire weather and indicated the extreme fire risk in 2020. When we focused on the state of California (not shown), we found that temperature and VPD in 2020 August exceeded 2σ level variability while precipitation was within 1σ variance level. In September, only VPD exceeded 2σ level and reached the highest value on record in 2020.

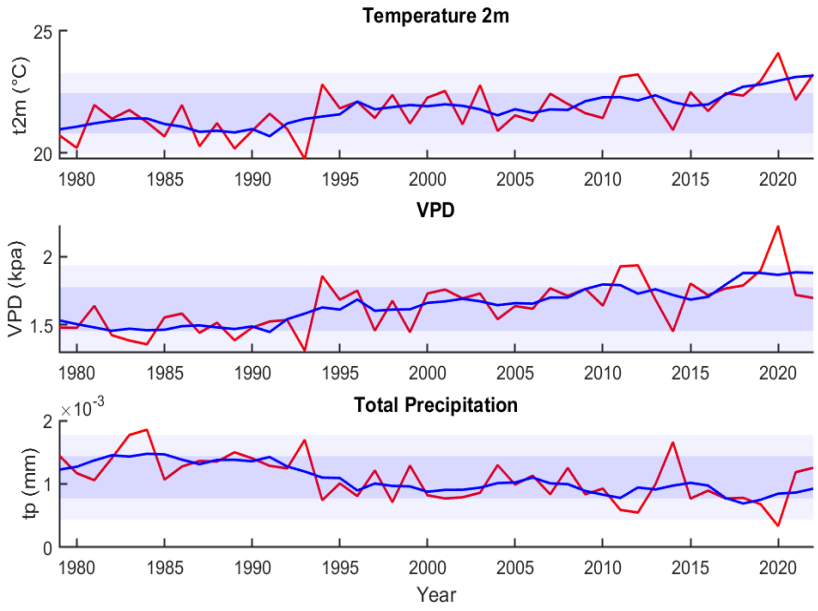

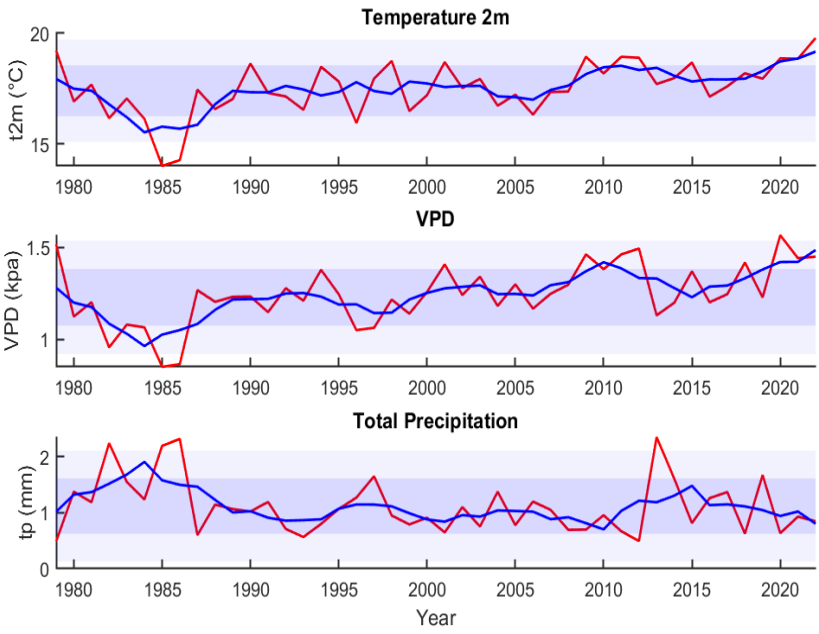

Figure 3.4 Emergence of changes outside of historical experience in observed climate factors, time series of mean annual variation in western US. (air temperature at 2m, VPD and precipitation). ±1σ noise level around the historical mean uses dark purple shading and ±2σ uses light purple shading. The upper panel is in August and lower one is in September.

In 2020, a significant portion of the Western United States experienced extreme heat and drought conditions, resulted in an exceptional level of hot and dry weather across the region, especially in August and September. Figure 3.5 illustrates a percentile map depicting various climate and weather variables associated with fire danger conditions across the western U.S. These variables include air temperature, VPD, RH, precipitation, vertical velocity at 500 hPa, specific humidity at 500 hPa, surface pressure and surface wind speed. The percentile calculation was based on the ERA-5 reanalysis monthly data from 1980-2020. In August, the percentile map reveals that

VPD, surface temperature and RH have reached historical record levels, indicating exceptionally hot and dry surface condition compared to historical data, over a great portion of the region including the southern part of California and Southwest states. Similarly, in September, extreme heat and drought continued across these regions, although the severity was somewhat reduced compared to the preceding month of August. The most notable feature in September was the positive surface pressure anomaly over the entire western U.S and strong sinking motion over the Great Basin associated with high-pressure anomaly, compared to historical levels. The strong sink motion of air would further heat the lower atmosphere and surface and bring drier air to lower level as shown in specific humidity figure. Another noteworthy feature during September is the historical record strength of easterly wind over the Cascade Range from Washington to California State. The downslope offshore winds accelerated the rate of wildfire spread in a remarkable combination of a pronounced absence of moisture and high thermal conditions, which occurred in the vicinity of the Oregon Cascades from September 7^{th} to 9^{th} (Abatzoglou et al. 2021).

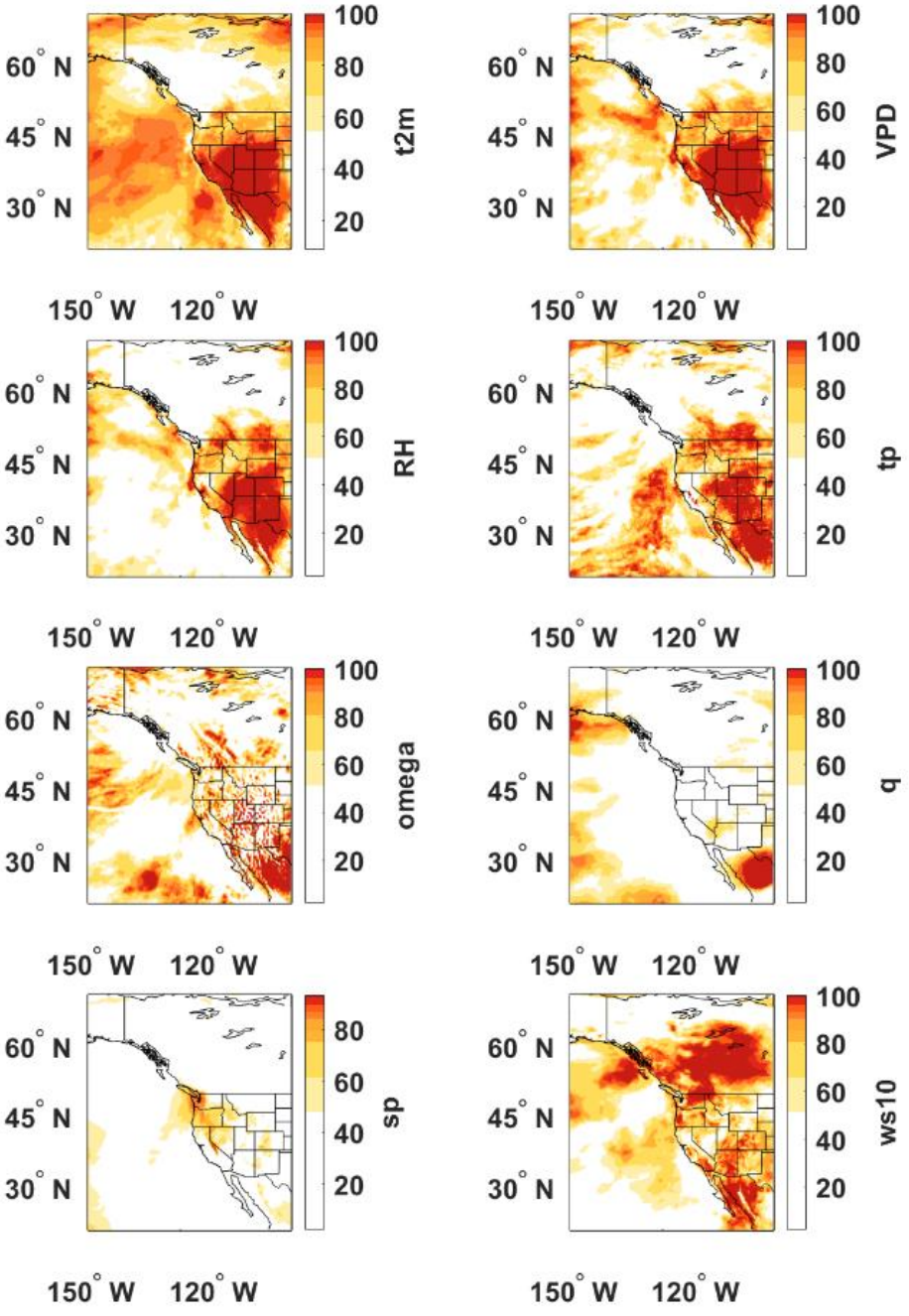
60° N
45° N
30° N
150° W
120° W
100
80
60
40
20
t2m
VPD
RH
tp
omega
q
sp
ws10

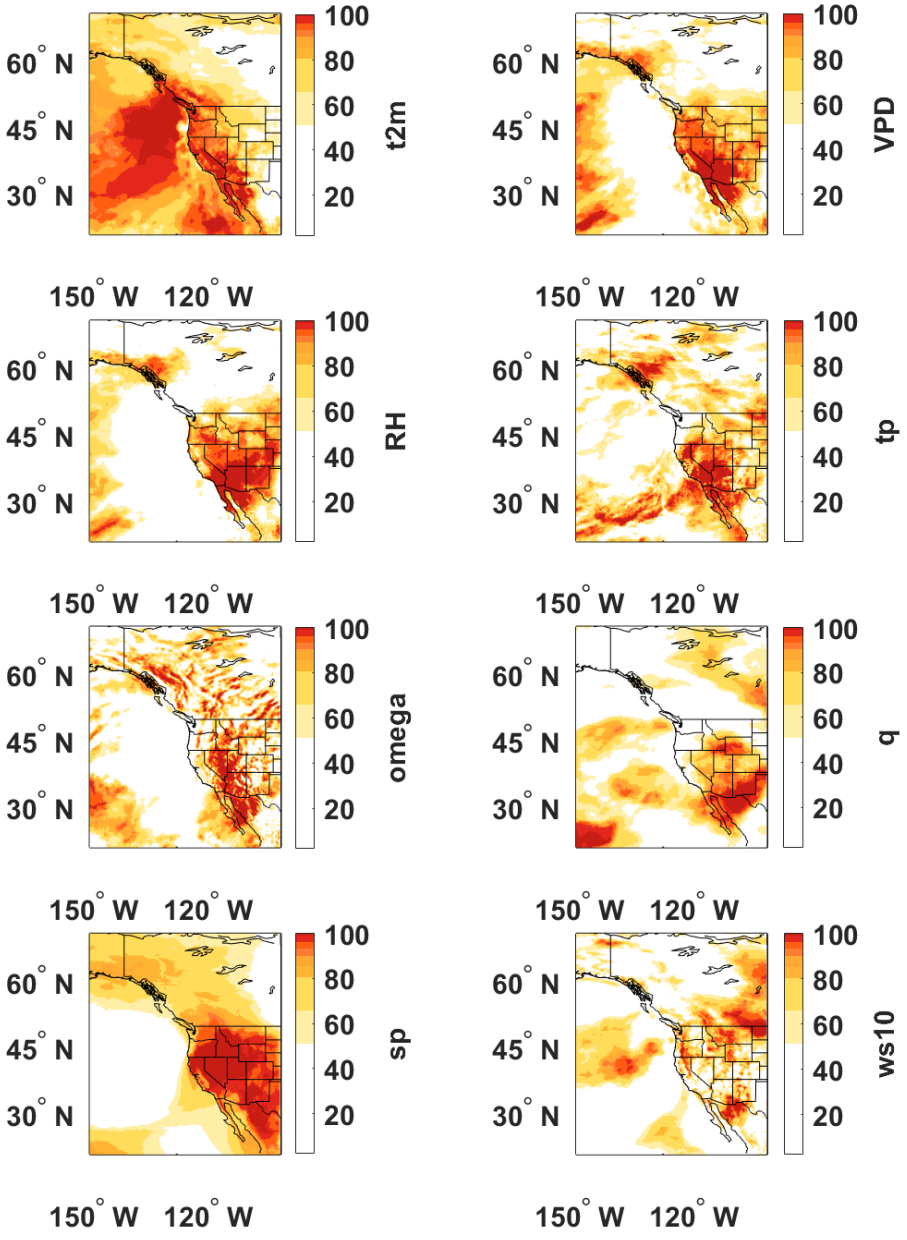

Figure 3.5 Spatial percentile map of climate and weather variables in August (upper panel) and September (lower panel) in 2020.

Among the various climate factors above that influence wildfires, temperature, VPD, RH and precipitation are considered as four of the most critical ones. Figure 3.6 shows the relationship between fire season (May to September) burned areas (fire number) with these four factors with linear regression from 2001-2020 in the western U.S. VPD explains 67% (64%) of variability in burned area (fire number) from 2001 to 2020, and 2020 ranking highest value in burned area (fire number) and VPD. When VPD levels are high, it can cause vegetation to lose moisture more quickly, leading to drier fuels that are more susceptible to ignition and more likely to contribute to the spread of wildfires. VPD is a better indicator RH in explaining the risk of wildfire activity because it considers the actual amount of moisture in the air, rather than just the relative amount of moisture compared to the maximum amount that the air can hold. Since VPD considers both temperature and RH, it provides a more direct measure of water stress on vegetation, thus it explains the burned area better than temperature (41%) or RH (49%) alone. Although total precipitation is an important factor in determining the moisture content of vegetation and fuels, it is not the best indicator of wildfire activity in the western US, as the relationship between precipitation and wildfire activity can be complex and can depend on a wide range of factors (Holden et al 2018)

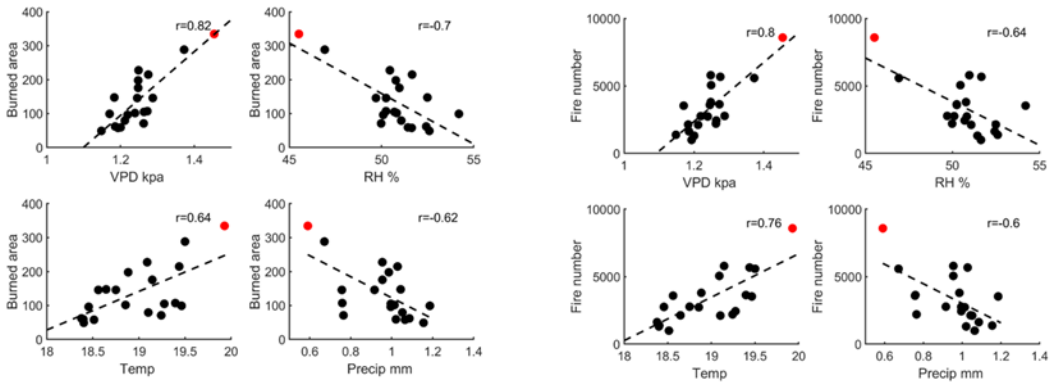

Figure 3.6. Scatter plot of burned area (left panel) and a) VPD, b) RH, c) temperature and d) Precipitation, with linear regression. Red dot represents year 2020. Similarly for fire number (right panel)

The previous analysis suggests that VPD is a more effective variable for explaining extreme wildfire behavior compared to temperature or precipitation alone. To better understand how annual VPD is driven by RH or temperature, we investigated the relative role of these two variables in affecting VPD. We defined 'T-driven VPD' as a scenario in which we hold the annual RH constant by using climatology spanning 40 years. In this scenario, the only variable allowed to vary is temperature. Similarly, we define "RH-driven VPD" as a scenario where we keep annual temperature constant using the same 40-year climatology, but this time we vary only relative humidity. These definitions enable us to examine and compare the individual impacts of temperature and relative humidity on annual VPD, respectively. Fig 3.7 shows the RH-driven VPD could capture the most peak and variability of the annual VPD during the 40-year period, which indicates the annual VPD variability is more sensitive to RH. The increasing trend of warm season VPD is over most of the western U.S., except for the northeastern western U.S in the past four decades (shown in Fig.3.8). The most

significant increasing trend occurs in the central-southern region of California. VPD is defined as the difference between the actual vapor pressure (e_a) and the saturation vapor pressure (e_s) at a specific temperature. We calculated the changes in e_a contribution to the VPD trend in Fig 3.8. Overall, the rise in e_s explains most (nearly 80%) of the total VPD trend, suggesting that the VPD increase is largely attributable to warming temperatures, which is consistent with previous findings (Zhuang et al 2021). However, it is crucial not to overlook the decline in e_a, especially over parts of California and the Southwest. In the central-southern region of California, the decrease in e_a explain over 40% of the VPD trend, indicating the important drying effects over these regions. A VPD trend study shows reduction in actual vapor pressure accounts for 40% of the observed increase of 53% of VPD over the Sierra Nevada and one-fifth of the total regional average increase in VPD of 57% over the Rocky Mountain (Chiodi et al. 2021).

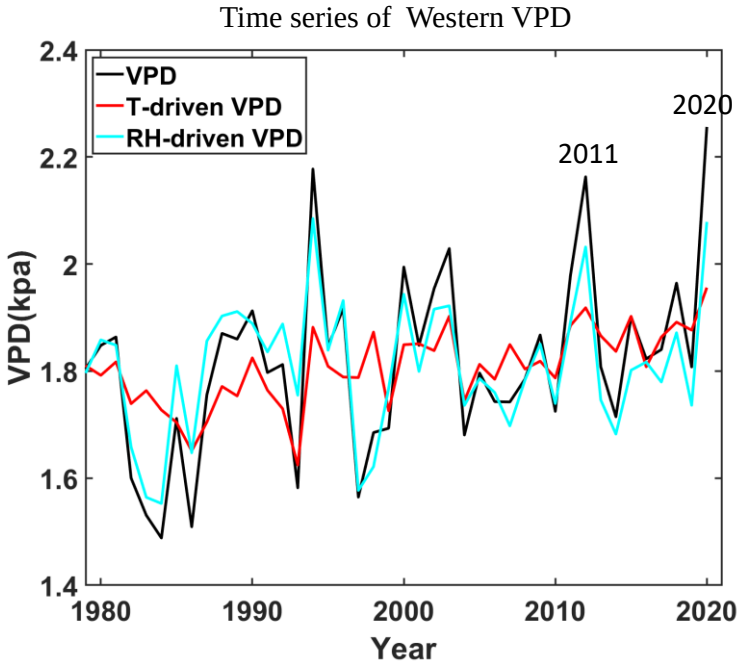

Figure.3.7 Annual VPD time series from 1979-2020 in western US.

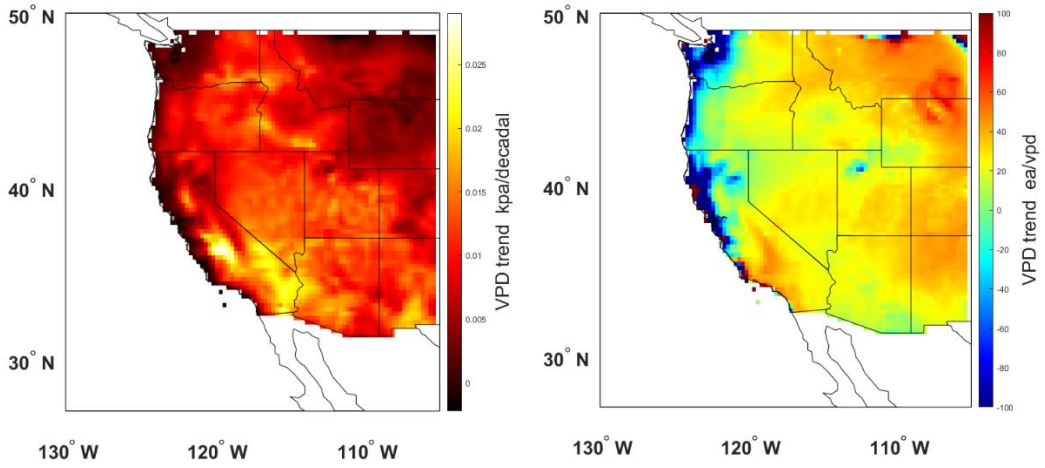

Figure.3.8 VPD trend (left) and contribution from e_a (right)

After analyzing the surface variables, the vertical profile of atmosphere is also important to be investigated. Figure 3.9 shows the vertical profiles of annual anomaly for RH, q (specific humidity) and T in 2020 September. There is an obvious trend of the atmosphere (200 hPa to surface) becoming warmer and drier during 2000-2020 compared to the period of 1979-1999. The RH hit the extreme low in 2020 from 300 hPa to the surface and similarly for q. For temperature, although it was very hot in 2020, it did not hit the record-high in the past forty years. This indicates that dryness is likely more important than hotness in regulating extreme wildfire events. Since RH is both regulated by temperature and humidity, it can be explained in term of the temperature-saturated water vapor constraint governed by the Clausius–Clapeyron (CC) relationship:

$$dR_h = \frac{dq}{q_s} - \alpha R_h dT$$

Where R_h is the relative humidity, q is the specific humidity, q_s is the saturated specific humidity, $\alpha = 6.5\% \ K^{-1}$, and T is the temperature. Based on this equation, the change of RH is dependent on two major terms: the first term is the dq/q_s and the second term is dT. The first term is more dynamic related, which depends on efficiencies of convection and atmospheric moisture transport. The second term is related to the thermodynamic warming effect. Under the effects of GHG forcing, the second term is usually negative (warming), leading to the decrease in RH. Additional RH deficit could occur due to dynamical effects as the first term (i.e., increased anomalous subsidence bringing drier air from above). In the case of the year 2020, we calculated the RH deficit based on the above equation and could separate the relative contribution of dq and dT. Usually, the warming term dominates the deficit of RH. However, in the case of 2020, we found that the dq term contributed nearly the equal or more portion of the decrease in RH than the dq term in the lower and mid troposphere over the western US, especially in the month of September and October. The anomalous deficit of moisture is mostly due to the anomalous subsidence and high pressure over the western US (Figure 3.5). Adiabatic warming of the descending air would also enhance the warming of the atmospheric column, further reducing RH as discussed in Chapter 2. Considering the evidence from CMIP5 simulations and reanalysis (Lau et al 2015;200), this scenario of anomalous subsidence and high pressure would be more frequent in the future over the western U.S.

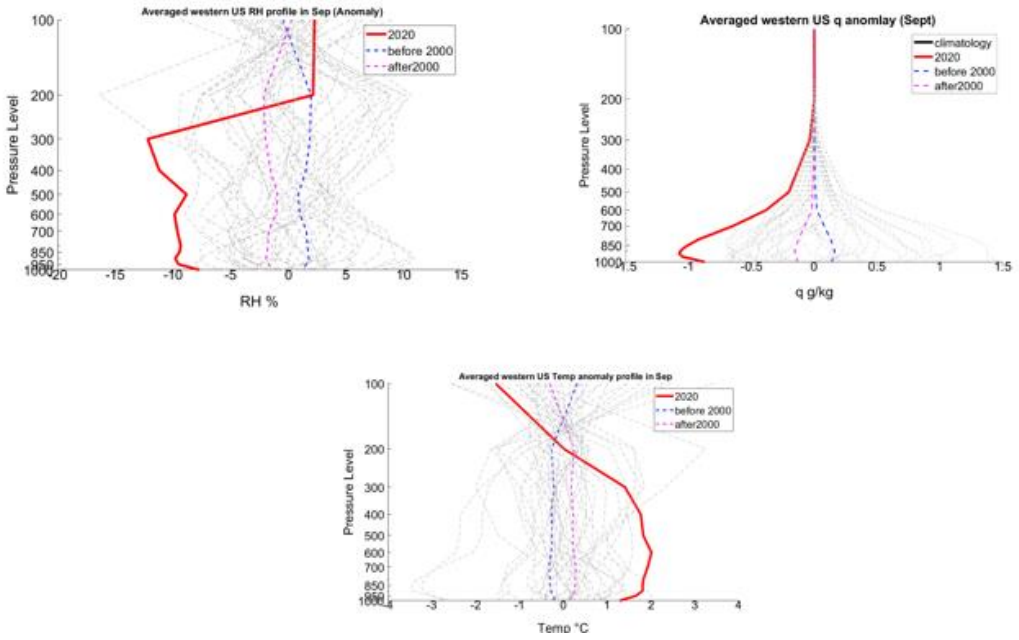

Figure 3.9 Vertical profiles of annual anomaly for RH, q (specific humidity) and T in September in the western U.S.

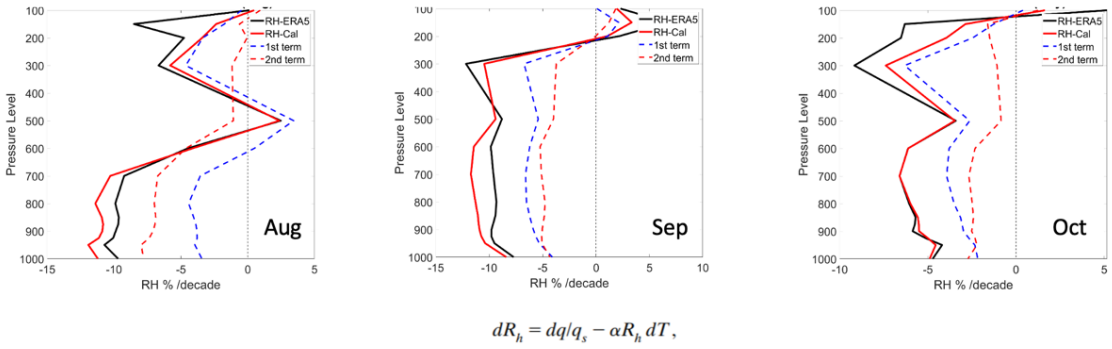

Figure.3.10 RH profiles based on ERA5 dataset and calculation from C-C equation.

The extreme anomalous subsidence in western US of 2020 September is shown in Fig.3.11. In the past 40 years, the vertical motion of troposphere has a positive trend

(sinking motion). For 2020, this sinking motion reached a record-high, creating extreme high pressure and bringing more dry air from above over entire western US, thus exacerbating the extreme dryness over the entire troposphere during this period. Figure.3.11 (b and c) show the extreme anomaly of geopotential height over the western U.S at 300 hPa and 700 hPa level.

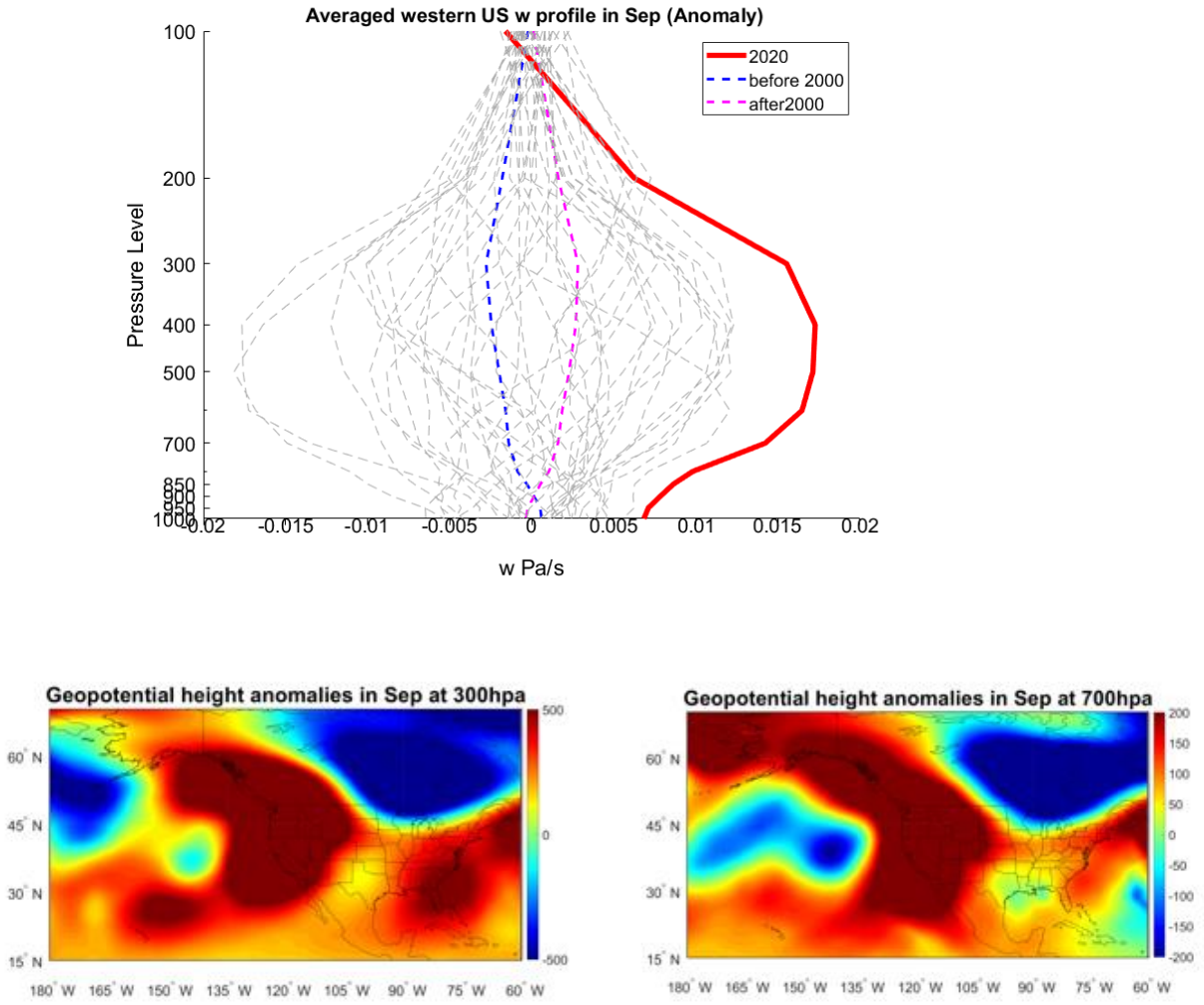

Figure.3.11 Vertical profiles of annual anomaly for sinking motion (a), and Geopotential height anomalies in September at 300 hPa and 700 hPa

3.3.3 The role of lightning and wind in 2020 fires

Lightning always plays a critical role in the initiation and propagation of wildfires in the western U.S. These lightning-started fires usually dominated the mountainous regions (Balch et al. 2017), whereas human-started wildfires occur in more-populated western coastal regions. For California, lightning-start wildfires are more prevalent over the northern mountainous part of the state. While human-caused fires are more frequent, lightning-caused fires often burn larger areas, primarily because they often start in remote locations where suppression efforts may be delayed, and lightning can ignite clusters of wildfires by striking multiple locations. Lightning strikes that occur during a thunderstorm but with little or no rainfall are categorized as dry lightning. These types of lightning strikes can pose a heightened risk of wildfires in the western U.S. Between 2020 August 16th and 17th, outbreak of thousands of dry lightning across Northern California combined with existing extreme dry conditions ignited the August Complex, SCU Lightning Complex, LNU Lightning Complex, and North Complex fires. These fires are ranked as the 1_{st}, 4_{th}, 6_{th}, and 7_{th} largest fires in California modern fire records, and over a million acres burned in second half of August 2020.

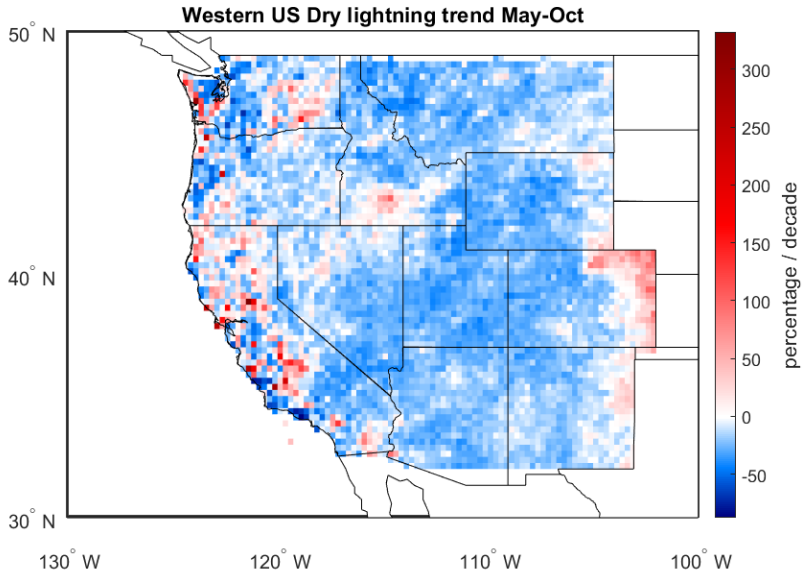

Figure 3.12 Dry lightning trend over western US from 1997-2020 in warm season (May-Oct)

Despite a significant dry lightning outbreak in mid-August, the total number of CG lightning strikes recorded for the entire month of August was lower than the climatological average. Dry lightning days in 2020 were also in the low level in the historical record in the past 30 years. According to the dry lightning spatial extent analysis (Kalashnikov et al.2022), the 10 largest daily lightning affect area in the recent 30 years were analyzed and 2020 Aug 17th ranked 9th in the record. Only three out of ten were associated with the large burned area, indicating that atmospheric dryness enabled fuel readiness is more important than lightning ignition number or extent. Figure 3.12 shows the dry lightning trend over western US from 1997-2020 in warm season (May-Oct). An overall decreasing trend has been observed in most of the western U.S, except for certain regions in California (North and Central part) and western costal area in Washington, consistent with other study regarding the declining

trend of dry lighting days in California (Kalashnikov et al. 2022). It is expected that areas witnessing a rise in dry lightning incidents will face a greater threat of wildfires in the future, given the projected increase in fire-prone weather conditions. For Human-ignited fires, most of western states experience the increased trend of fire number except for California.

Wind also plays a critical role in the spread and behavior of fires in the western US. The 2020 wildfires in this region were exacerbated by more than just heat and dryness. An offshore wind event, which occurred in early September resulted from an atmospheric wave train that spanned the Pacific Ocean (Allen et al.2020), was also a significant contributing factor. Between 2020 September 7-9, there were downslope offshore winds that swept across the Oregon Cascades, resulting in extremely powerful winds and arid conditions that caused wildfires (Labor Day fires) to spread quickly. An omega block situated off the coast of British Columbia, combined with a cut-off low-pressure system near the Four Corners region, created favorable conditions for northeasterly strong wind patterns. Fig 3.13 shows daily wind speed percentile for September 8th, 2020, across the western United States. Cascades ranges experienced record-high wind speeds on this day. RAWS station at Gellatly Oregon shows this strong wind event started from afternoon of September 7^{th} to the morning of 9^{th}, accompanied by an extremely reduced level of RH (less than 20%), creating most favorable conditions for wildfires spread. Although robust easterly winds have typically occurred in early September across the Pacific Northwest and have been linked with the most substantial fires west of the Cascade Mountains (Reilly et al., 2022), the 950 hPa winds recorded in September 2020 were the strongest observed for

that time of year in many locations, according to observational records (Abatzoglou et al. 2023; Russel et al. 2024). Recent studies reported a slight decline in surface offshore wind over much of Oregon and California in autumn, while an increase in annual downslope wind activity was found across Pacific Northwest (Abatzoglou et al 2023). A 25% increase in the annual downslope wind-driven fires number and a 140% increase in burned area were documented in the western U.S during 1992–2020, which partially reflects trends toward drier fuels enabled by climate change.

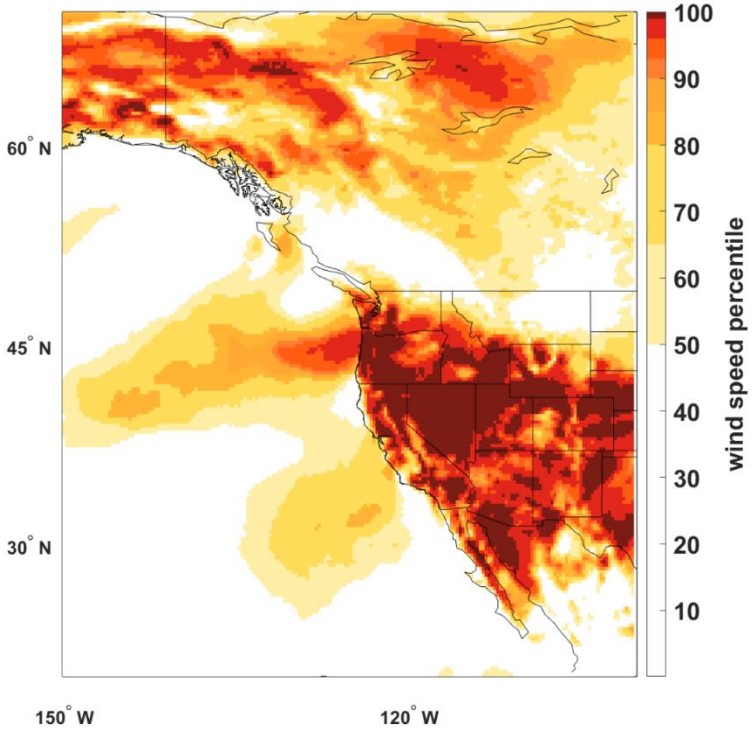

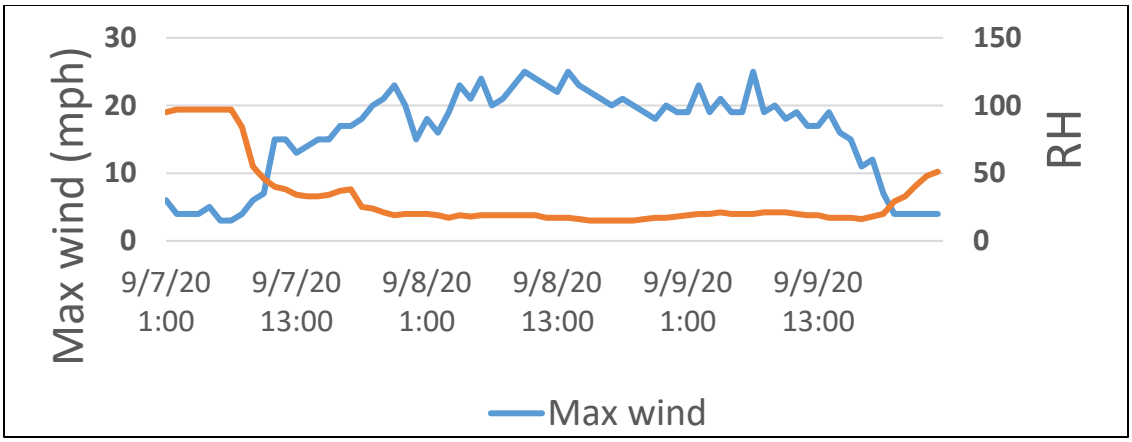

Figure 3.13 Daily wind speed percentile for Sep 8 in 2020 across the western U.S.(upper panel) and recorded max wind and RH changes from RAWS station at Gellatly Oregon (lower panel).

3.4 Discussion and conclusions

The exceptional 2020 fire season in the western U.S was the result of a combination of multiple climate and weather extremes, akin to the formation of a "perfect storm". This year's widespread burning was most significant during the months of August and September. In August, the burned area exceeded the annual average by over four times (primarily from CA), while in September, it surpassed the climatology by more than five times (from Pacific Northwest). Record-setting climate including atmospheric aridity and elevated temperatures reflected by VPD, enabled this extraordinary 2020 fire season in the western U.S. The unprecedented high VPD directly increases fuel aridity, rendering the vegetation more susceptible to ignition and facilitating fire readiness. In mid-August, this extreme fire risk was accompanied by a rare outbreak of CG dry lightning across Northern California, leading to the most wildfire season in the recent California fire history. In September, compound extremes exacerbated the fuel

aridity since August. Historic offshore wind events in early September fanned numerous human ignited fires and spread rapidly across the northwestern U.S. August and September experienced remarkable fuel dryness, as indicated by the Vapor Pressure Deficit (VPD), driven by climate and weather extremes. However, the mechanisms behind the fuel drying differed between these two months. In August, the record high VPD was primarily due to exceptionally high surface temperatures. Conversely, September saw record-high pressure and descending air motion throughout the troposphere, coupled with high temperatures, contributing to the extreme VPD. It's worth noting that we observed dynamic-related factors accounting for over 50% of the tropospheric Relative Humidity (RH) deficit, underscoring the significance of subsidence linked to atmospheric and surface dryness.

It is noteworthy that other factors are also important to the escalating burned area in the western U.S. Poleward-shifted and waiver polar jet stream would enhance fire-favorable surface weather conditions in this region (Allen et al. 2020). La Niña climate pattern would bring a drier Southwest and perhaps a more fire-prone California although in 2020 it started in late September.

Chapter 4: Evaluation and improvement of fire weather indices over the western U.S.

4.1 Introduction

The assessment of fire risk is conducted on a daily to seasonal basis through various indices that are derived from meteorological data. These indices describe the probability and potential severity of wildfires and are operationally employed to assist fire managers in evaluating risks to vulnerable areas and in prioritizing their firefighting strategies. Different fire management systems are used in different locations. Fire management practices vary by location, employing different systems. For Canada and Alaska, Fire Weather Index (FWI) system, a key part of the Canadian Forest Fire Danger Rating System (CFFDRS), is commonly utilized. The FWI evaluates daily fluctuations in the likelihood of wildfires, and it is specifically designed for use in boreal ecosystems. In the contiguous United States, the primary tool for managers to estimate the risk of wildfires is the National Fire-Danger Rating System (NFDRS). Both systems consider weather conditions, but the NFDRS also integrates local factors like topography (slope) and fuel types (fuel model) more comprehensively. The Fire Weather Index (FWI) requires fewer inputs compared to the National Fire-Danger Rating System (NFDRS), making it more suitable for areas with limited data availability, such as Alaska.

A lot of previous studies have compared various fire danger rating systems or fire indices to assess their suitability for specific purposes. Lee (2019) evaluated four systems utilized in Canada and discovered that each of these systems excelled in

distinct tasks, with all of them providing valuable information for making management decisions. The recent study compared 13 indices over Alaska region with MODIS fire data and concluded that Duff Moisture Code (DMC) and Buildup Index (BUI), along with atmospheric forcing indicator vapor pressure deficit (VPD), demonstrated superior performance in capturing the conditions favorable for significant wildfire incidents (Ziel et al. 2020). A comparison of NFDRS with recorded fire occurrence was conducted across entire conterminous US from 2006-2013, revealing the higher correlation in in the Northwest, Northern Rockies, Great Basin and Northern California than areas in the Southern and Eastern US (Walding et al. 2018). However, this analysis based on monthly mean fire danger indices and monthly fire occurrence and size is too coarse for the evaluation. The recent availability of data for NFDRS components and indices from ECMWF Reanalysis v5 (ERA5) makes it possible to compare with indices from CFFDRS over longer time periods and at higher temporal resolution. In addition, an evaluation based on conditional frequency distributions analysis would be applied instead of using simple correlation method. The significant gap in the literature leaves a crucial question unanswered: how these two prominent fire danger-rating systems, each with its unique methodologies and applications, are compared against each other in terms of their effectiveness and reliability in assessing fire danger over the western U.S.

One limitation of these indices is that all inputs are based on only surface meteorological and fuel information, without considering the lower atmospheric dryness and instability, which could play an important role in developing very large fires. The behavior of extreme fires is often related to the interaction of the wildfire

dynamics and the surrounding atmosphere, especially for the type of convective fires, when convection is an important driver of the fire spread. The Haines index (Haines 1988) is specifically designed to assess the potential for wildfire growth by measuring the stability and dryness of the lower atmosphere, and have been used many regions of the globe such as United States (Trouet et al. 2009), Australia (Mccaw et al.2007) and the Mediterranean basin (Tatli and Turkes 2014). Therefore, another goal of this work is to provide an enhanced version of the fire index to take into account atmospheric instability by combining the original fire index and Haines index together.

4.2 Data and method

4.2.1 MODIS Burn area and fire counts dataset

We used MODIS Burn area and Active Fire Product to represent wildfire activity and evaluate the performance of all indices. Details of MODIS fire product have been introduced in the previous chapter. This study used over millions of individual MODIS fire detections, each identified by date and time, over a 20-year period from 2001–2020. The MODIS count represents the quantity of detections recorded on each of those specific days. Our study regions are classified as eight ecoregions according to the level II Ecoregions from United States Environmental Protection Agency (EPA).

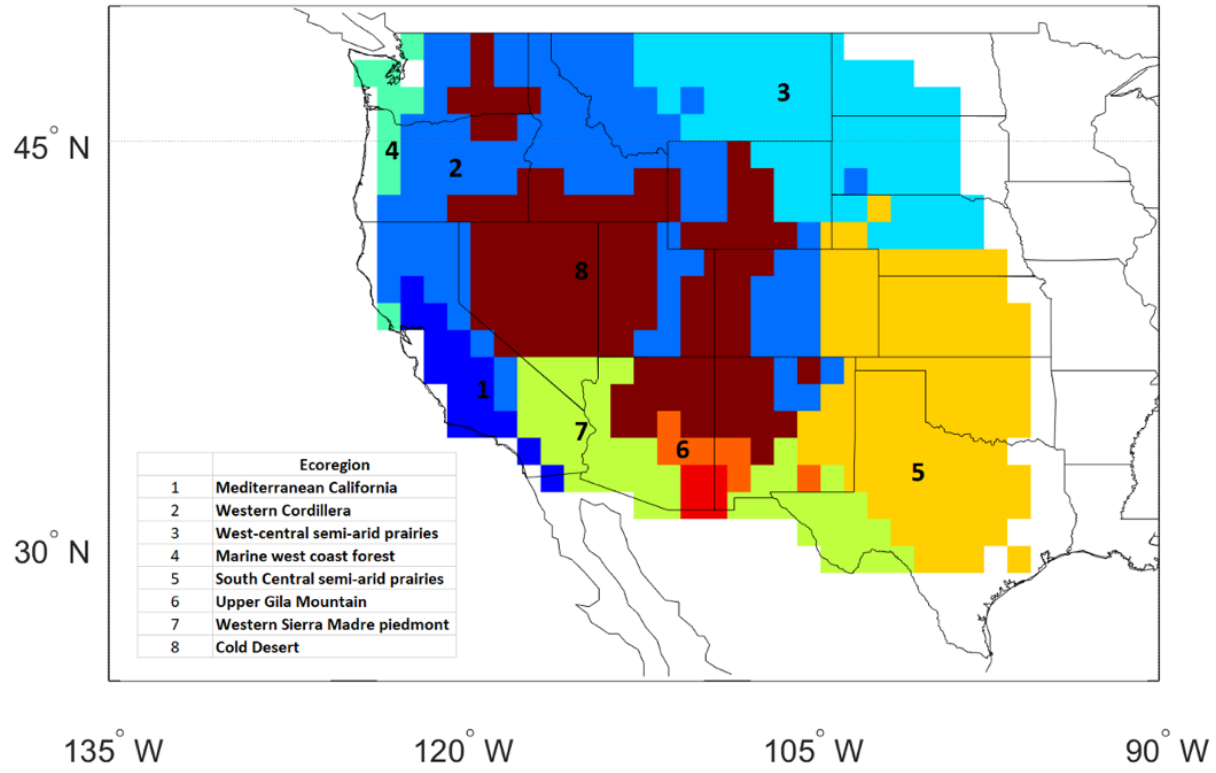

Figure 4.1 Maps of ecological region of western U.S.

4.2.2 Fire indices derived from ERA reanalysis data

The Canadian FWI quantifies the accumulated drying and potential flammability in its three fuel moisture codes and one fire behavior index.

The current standard indices of CFFDRS include Fine Fuel Moisture Code (FFMC), Duff Moisture Code (DMC), The Drought Code (DC), Initial Spread Index (ISI), Build Index (BUI), the Fire Weather Index (FWI) and Daily Severity Rating (DSR). The first three indices rate moisture in three fuel layers of varying depth: FFMC (litter and fine fuel at surface layer), DMC (loosely compacted organic layers at moderate depth) and DC (deep, compact organic layers). The remaining four indices are fire behavior related indices include BUI, ISI, FWI and DSR. BUI is based on the DMC and the DC, rating

the total amount of fuel available for combustion. ISI rates the rate of fire spread based on wind speed and FFMC. FWI is used as a general index of fire danger, combing ISI and BUI. DSR is based on the FWI but more accurately reflects the difficulty of controlling fires.

The Vapor pressure deficit is already introduced in Chapter 2 and 3, defined as the difference between the amount of moisture in the surface air and how much moisture the air can hold when it is saturated. Essentially, it indicates the drying capacity of the air.

The National Fire Danger Rating System (NFDRS) in the United States has four fire indices output including the Spread Component (SC), Burning index (BI), Ignition component (IC) and Energy Release Component (ERC). They evaluate the severity of burning conditions and the risk of wildfires. SC is a numerical value representing the expected forward speed of a fire's front in feet per minute. This component is influenced by factors like fuel model properties, moisture in living fuels, moisture in 0 to 3-inch dead fuels, wind speed, and slope. Its variability is closely linked to changes in relative humidity, wind, and moisture in living fuels. IC reflects the likelihood for a fire to ignite that requires suppression activities. BI serves as a gauge of the potential difficulty in controlling a fire, based on its predicted intensity and speed. It is derived from the SC and ERC and shows moderate variability. This index is particularly sensitive to different fuel models and can effectively track seasonal trends, especially in models with substantial dead or live fuel content. Its accuracy, however, is greatly affected by errors in weather observations, such as wind speed and relative humidity.

The hot-dry-windy index (HDWI) is a new fire weather index formulated to account for meteorological conditions both at the Earth's surface and in a 500-m layer just above the surface (Srock et al 2018). As the name suggests, it integrates three critical weather factors that influence fire behavior: temperature (hot), humidity (dry), and wind speed (windy). It is proposed to replace the Haines index in the US as showing better accuracy for severe fire occurrences.

The Haines index is used to indicate the potential for wildfire growth by measuring the stability and dryness of the air over a fire. It is calculated by combining the stability and moisture content of the lower atmosphere into a number that correlates well with large fire growth. The stability term is determined by the temperature difference between two atmospheric layers; the moisture term is determined by the temperature and dew point difference. Because of significant elevation disparities across the United States, the index is computed across three distinct pressure ranges to account for varying elevations, from low to high.

Table 4.1 List of fire indices in our studies

Canadian Forest service Fire weather index rating system	U.S. Forest Service National Fire-Danger Rating System	Other
Fire weather index (FWI) Build up index (BUI) Drought code (DC) Duff moisture code(DMC) Fine fuel moisture code (FFMC) Fire daily severity rating(DSR)	Spread component (SC) Energy release component (ERC) Burning index (BI) Ignition component (IC)	Vapor-pressure deficit (VPD) Hot-Dry-Windy Index (HDWI) Haines (HI)

4.2.3 Frequency Distribution Analysis

This study involved a thorough analysis and comparison of data based on their frequency distributions. Specifically, frequency distributions were calculated for the number of fires detected by the MODIS, and these were used as the baseline to assess the effectiveness of various fire indices in predicting fire occurrences. However, a direct comparison of frequency distributions between the fire indices and MODIS data would not be suitable. This is because there can be instances of high fire risk weather conditions without actual fire occurrences, which could lead to an unfair assessment of the fire indices performance. To address this, conditional frequency analysis (Ziel et al 2020) was employed in this study. This method relates the frequencies of different levels of fire danger indices to wildfires are present or absence in the area. In practice, We calculate the frequency of different ranges of each fire index during MODIS counts and then divided by the total number of days in the record that met those same fire index thresholds These conditional frequency distributions were then compared with the observed frequencies of days when MODIS detected fires. The rationale behind this approach is that an effective fire index should show a frequency distribution closely matching the pattern of actual wildfire occurrences. The accuracy of each fire index was evaluated by calculating their cumulative deviation from the MODIS Day distribution, providing a measure of their effectiveness in reflecting fire weather conditions.

4.3 Result

4.3.1 Observed fire history over western U.S.

Figure 4.2 shows the annual and seasonal variation of MODIS fire counts for each ecoregion from 2001-2020. The ecoregions of Mediterranean California and Western Cordillera have the most fire counts among all. Most ecoregions have the increase trend of five activity during the past two decades. The seasonal variation indicates that the fire season for western US, which usually starts from May to October, peaking in August. Figure 4.3 shows the comparison between annual burned area and active fire counts from MODIS observations over California from 2001-2020. These two products show good agreement and therefore we use active fire counts only in the following discussion.

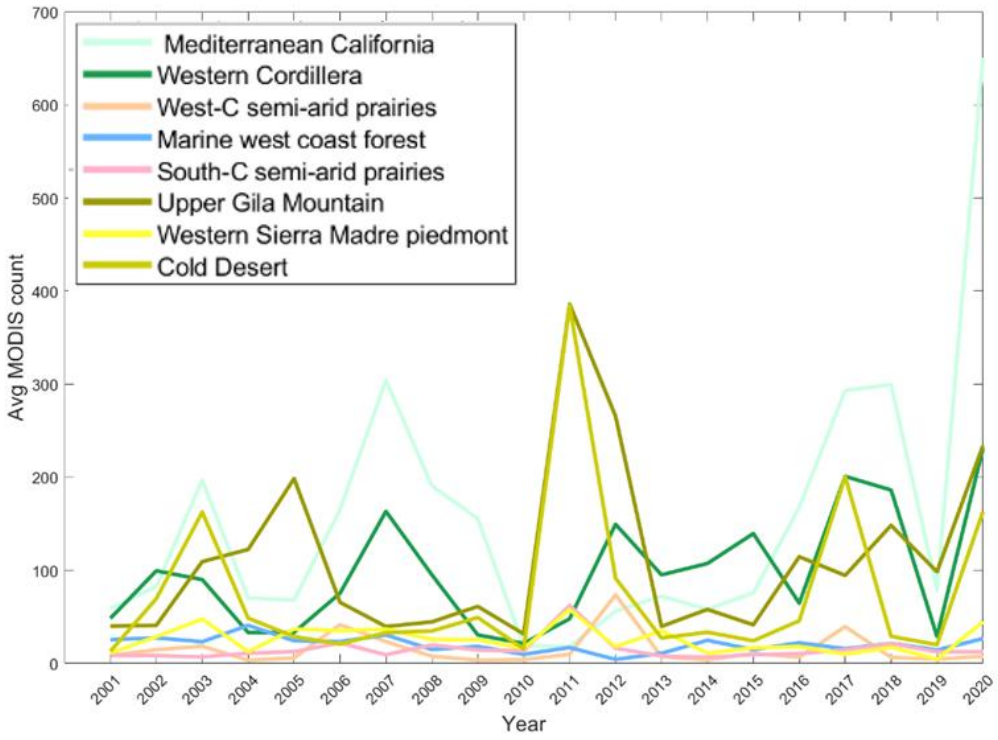

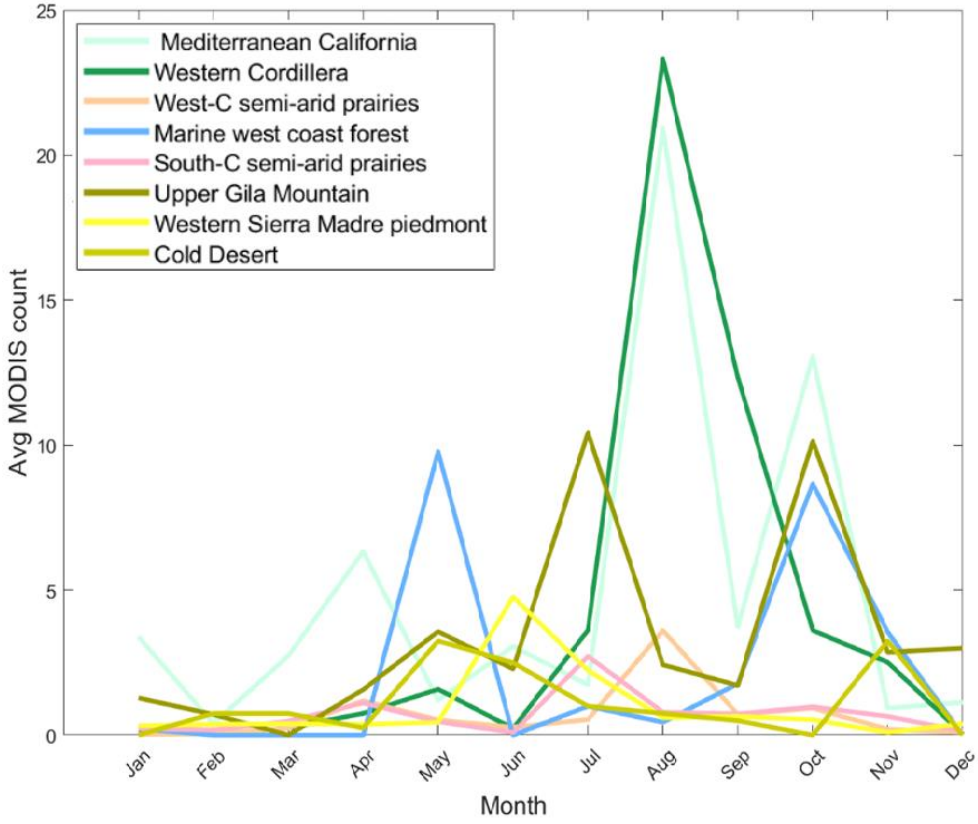

Figure 4.2 Annual (upper) and seasonal (lower) variation of MODIS fire counts for each ecoregion from 2001-2020.

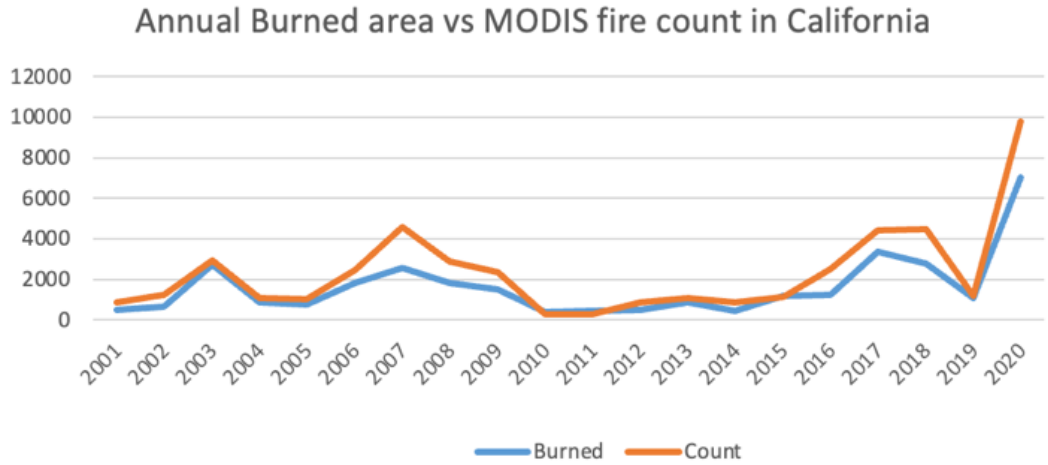

Figure 4.3 Time series of MODIS annual burned area and fire count from 2001-2020

Figure 4.4 shows the distribution across the percentile ranks of MODIS Count for each ecoregion over the western US. According to this analysis, over 95% of active fire counts occur in the top 10% of all days in the 20-year period. The underlying assumption of this study is that the noticeable increase in fire activity is primarily due to drying conditions in the atmosphere and on the ground, which in turn increases the flammability of landscapes. We will use these frequency distributions as benchmarks to compare and evaluate the fire indices against actual fire record.

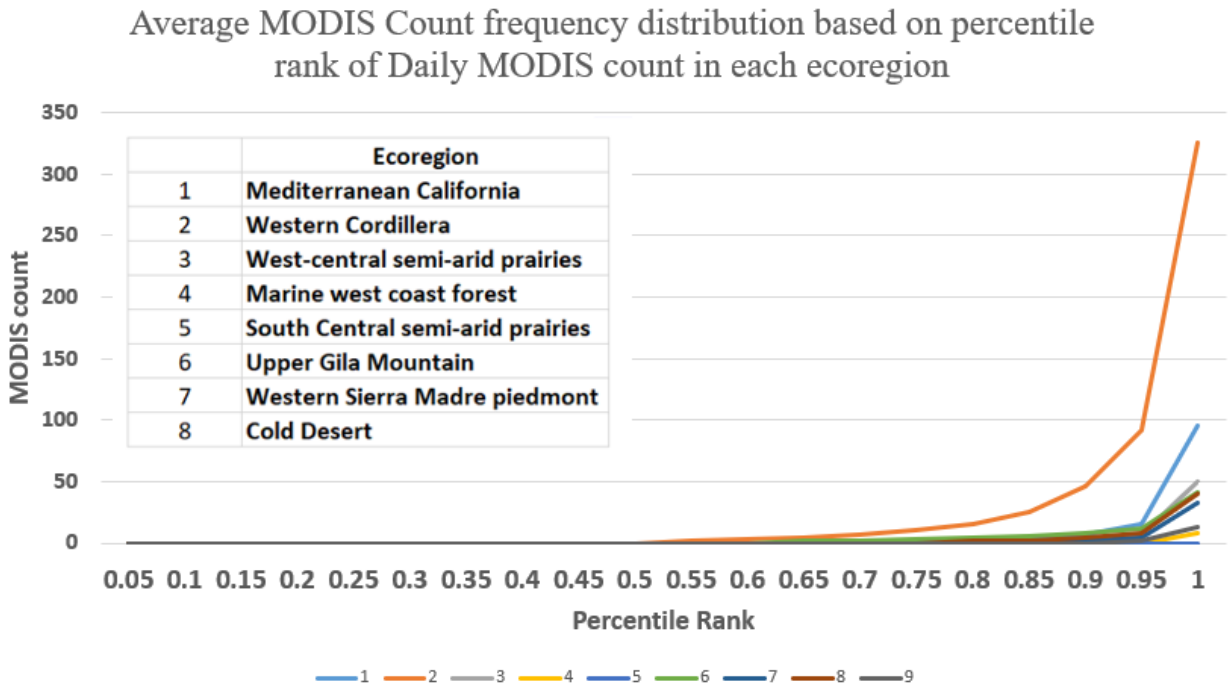

Figure 4.4 Distribution of active fire history over the 20-year study period.

.

4.3.2 Fire indices

Conditional frequency distributions were produced for each of the fire weather indices in each ecoregion for evaluation. The efficacy of using this method is explained and demonstrated below using an example of FWI in Figure 4.5. All day history (black lines), distribute all days in the 20-year record for each ecoregion varying all bins of FWI values and represent the overall frequency that each level of FWI occurred in the record, regardless of fire occurrence. MODIS Count (yellow line) distributes all of the MODIS active fire counts across the same FWI scale, showing that very little fire activity when FWI has low value. The intermediate FWI value here is associated with the most fire counts shown by the MODIS count distribution. The conditional frequency distribution better formalizes the comparison by examining the frequency of MODIS detections. The conditional frequency is calculated by dividing their raw (MODIS history) frequency at each point along the FWI scale by the All-Days (index history) frequency at each point. This could provide the frequency at which MODIS Counts occurred in the record relative to those when no fire activity was present at each level of FWI. With this transformation, it is clear that as FWI increases, the likelihood of significant fire activity (MODIS Counts) increases as well. For all indices and all ecoregions, we applied the same method of conditional frequency distribution as shown above.

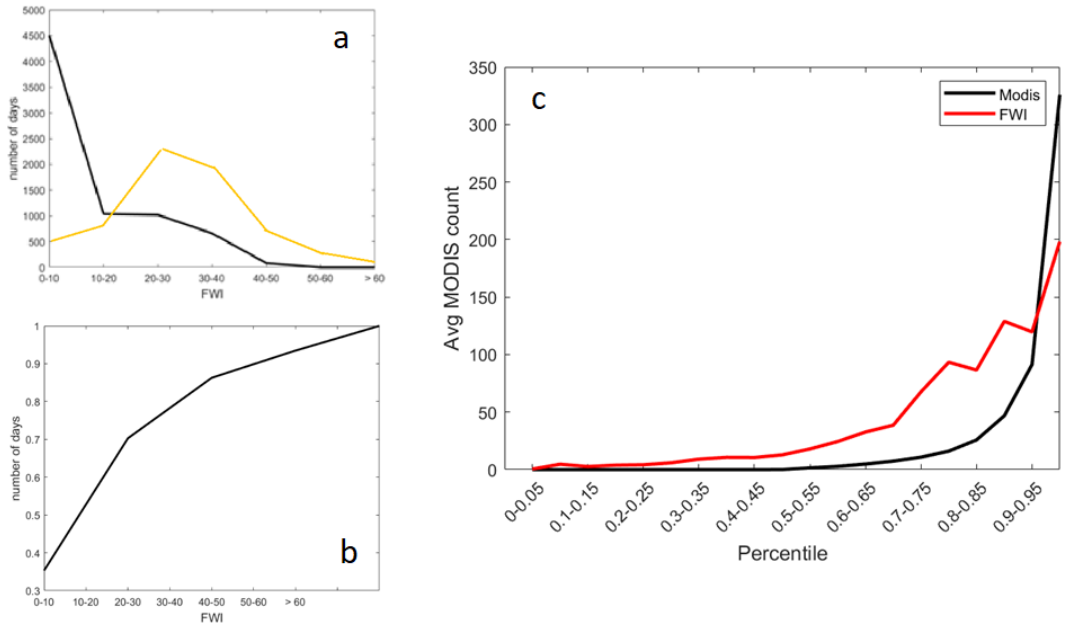

Figure 4.5 Frequency distribution MODIS Days scaled by FWI. (a) Raw data (black) all day, MODIS days (yellow). (b) Conditional frequency distribution scaled by FWI. (c) Conditional frequency distribution scaled by FWI percentile ranking.

4.3.3 Fire index performance

Figure 4.6 presents the cumulative departures ranking (a) and monthly correlation (b) for the conditional frequency distribution of each fire index in relation to the underlying MODIS Counts history for different regions of western US. In Figure 4.6, the cumulative departure values have been transformed into the ranking number. For example, rank No.1 indicates the least cumulative departure (a) or best correlation (b) compared with fire activity (best performance). For conditional frequency cumulative departure, the performing ranking of the indices are DMC, BUI and FWI for Rocky Mountain region (Western cordillera), while for Mediterranean California, they are HDWI, FFMC and FWI. In general, the indices from CFFDRS (Canada) have better performance than the indices from NFDRS (US) in the high fire active region,

especially in the region of Mediterranean California, Western Cordillera and west-central semi-arid prairies. In addition, the relatively new index HDWI reaches 1st rank in three ecoregion (two along the western coast). Noted that including wind input, the HDWI index has much better ranking when compared to VPD index.

The monthly correlation figure shows the VPD related group (VPD, VPD at 700 hPa and HDWI) has the dominating advantage over other indices over nearly all ecoregion types. This is understandable as the month correlation is more related to the climate influence rather than weather impacts, and VPD has been proved the very close relationship with long-term fire trend over the western U.S.

Conditional frequency cumulative departure

Ecoregion	BUI	FWI	BI	DC	DMC	DSR	FFMC	ERC	IC	SC	VPD	VPD700	HDWI
Mediterranean California	12	3	9	13	11	4	2	6	7	10	5	8	1
Western Cordillera	2	3	10	12	1	4	5	6	11	13	9	8	7
West-central semi-arid prairies	13	8	10	2	12	9	3	4	6	11	5	7	1
Marine west coast forest	12	9	5	13	11	8	6	7	4	3	2	10	1
South Central semi-arid prairies	6	5	4	13	3	2	10	1	8	7	11	12	9
Upper Gila Mountain	12	7	4	8	13	5	1	3	6	2	10	11	9
Western Sierra Madre piedmont	12	9	2	5	13	8	7	3	6	4	10	1	11
Cold Desert	12	10	5	6	13	9	7	2	4	1	8	3	11

Monthly correlation

Ecoregion	BUI	FWI	BI	DC	DMC	DSR	FFMC	ERC	IC	SC	VPD	VPD700	HDWI
Mediterranean California	9	5	11	13	7	4	8	12	6	10	2	1	3
Western Cordillera	5	2	8	13	6	3	12	9	7	10	1	11	4
West-central semi-arid prairies	2	6	9	12	1	3	11	5	8	10	4	13	7
Marine west coast forest	8	11	6	13	5	4	9	10	2	3	12	1	7
South Central semi-arid prairies	4	10	9	11	2	5	12	6	7	8	3	13	1
Upper Gila Mountain	11	2	6	13	12	3	9	8	5	7	4	10	1
Western Sierra Madre piedmont	2	11	6	13	1	10	12	5	7	9	3	8	4
Cold Desert	11	3	6	13	12	1	10	9	7	4	8	2	5

Figure 4.6 Rank table for the performance of each fire indices for each ecoregion a) conditional frequency cumulative departure b) Monthly correlation.

4.3.4 Improved index incorporating Haines index.

Several studies have indicated the additional input from lower atmospheric information (drying and stability) could improve the fire danger forecast (Pinto et al.

2020; Santos et al. 2022). The indices above in our study are generally focused on the surface condition, which lacks the useful information of lower atmosphere. Therefore, we would like to combine the lower atmosphere information and origin index to a new combined index. For the lower atmosphere information, we will use the Haines index which could provide the lower atmospheric drying and stability condition. Firstly, we use the machine learning random forest method to determine the feature importance of different indices over two ecoregions (California and Rocky Mountain regions). We selected these two ecoregions as the regions with the highest occurrence of wildfires. Based on the output values of feature importance, we will calculate the weighting for our new combined index. For the new combined index, we use the Haines index and the index ranked 1st in machine learning. The Combined index = weighted importance * 1^{st} rank feature (normalized) + weighted importance * Haines index (normalized). Figure 4.7 shows that for the Rocky Mountain region, the 1st rank index is DMC, then we combine the DMC and Haines index in our new combination index. Similarly, for Mediterranean California, we will choose HDWI as the 1st rank index based on machine learning output. Noted that the machine learning output is generally consistent with the conditional frequency distribution analysis for these two ecoregions. We calculated the cumulative departure for the new combined index and found that the new index has the best performance (1^{st} Ranking) in the cumulative departure analysis, outperforming all other indices for both ecoregions. This indicates the importance of adding lower atmosphere stability regarding fire danger rating.

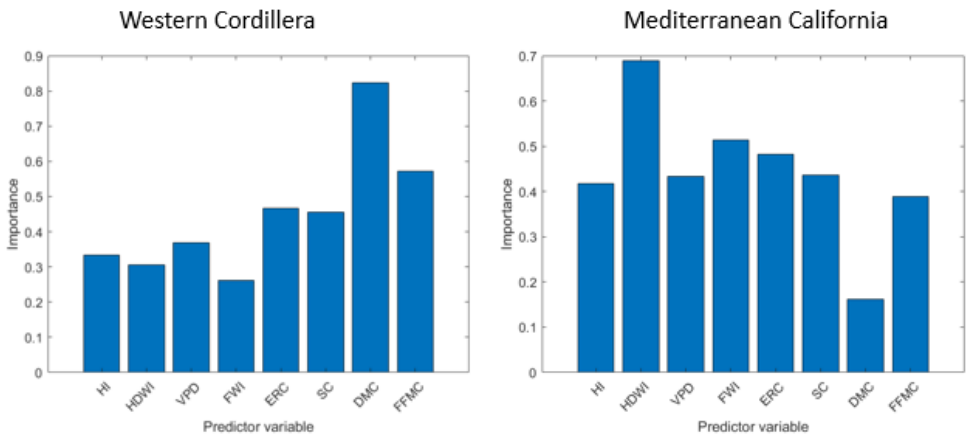

Figure 4.7 Feature importance based on the random forest machine-learning algorithm for a) Western Cordillera. b) Mediterranean California.

4.3.5 Validation with large fire cases in California

The cumulative departure analysis for conditional frequency provides the statistical base for our new combined index. To further prove its effectiveness in the fire-danger rating, we apply it in the actual fire cases and compare it with other advanced fire indices. In this study, we choose California for the study area and according to the above analysis, we choose the 1st rank index (HDWI) to test the performance of our new combined index. We selected several of the largest fires in California fire history in the recent 20 years. The first case is the Cedar fire in 2003. The fire started on 23 October and spread rapidly toward the west, with the largest spread day occurring on 26 October as a Santa Ana wind event developed (Raphael 2003). Both the HDWI and HDWI-HI (new combined index) indicate a clear maximum on the day when the fire was most difficult to manage.

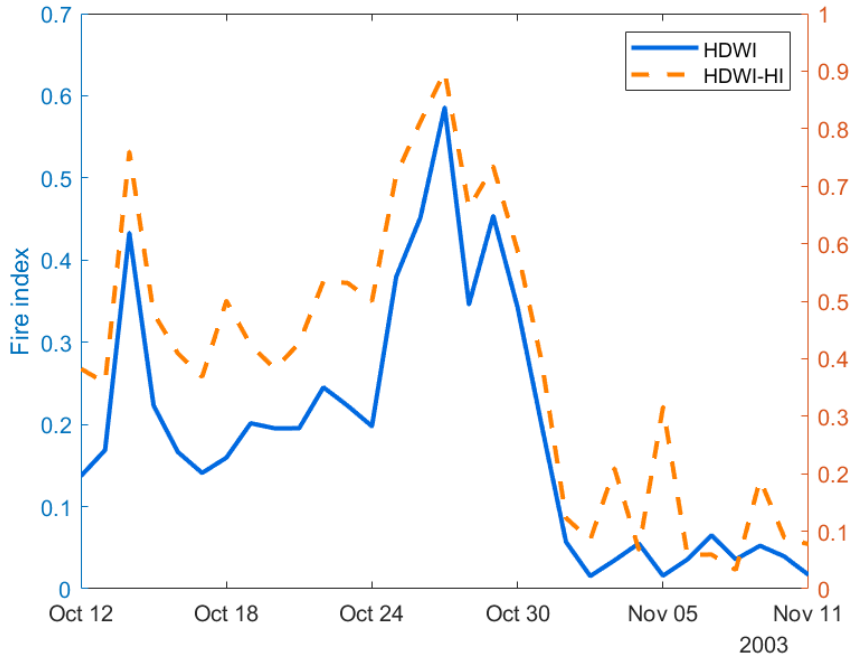

Figure 4.8 Case of Cedar fire in 2003

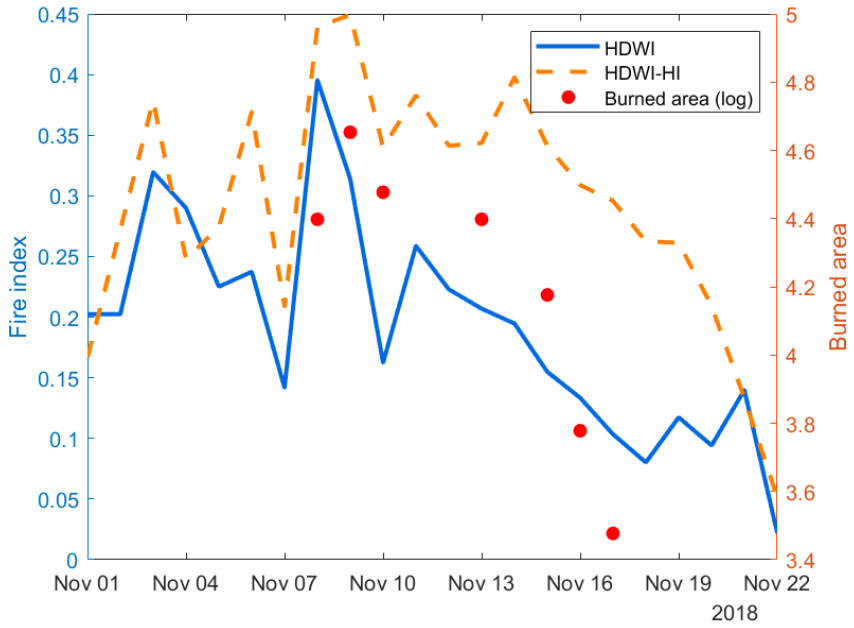

Figure 4.9 Case of Camp fire in 2018

The second one is Camp fire in 2018. The fire started on Nov 8 and the first 24 hours were characterized by a fast-moving fire with initial spread driven by high winds up to 22 m/s and long-range spotting up to 6.3 km into the community. The red dot indicates

the burned area daily from local fire record. The HDWI dropped quicky after the first fire day while the HDWI-HI still maintain the high value until Nov 15. In this case, the new index seems to have better agreement with actual fire development.

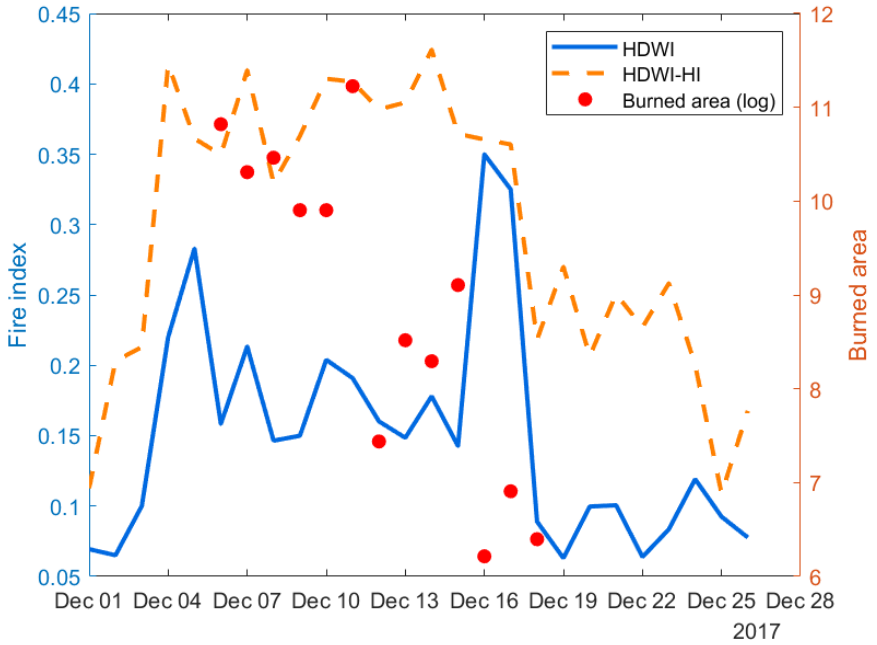

Figure 4.10 Case of Thomas fire in 2017

Here is the Thomas fire in 2017. The fire started on Dec 4 and largely weakened due to Santa Ana winds in the evening of Dec 17. It is clear that HDWI index had a false peak during Dec 16 and was affected too much by wind information, while the new combined index does not show such false peak. On December 10, the Thomas Fire had been generating its own weather for the past two days, a behavior only observed in very massive wildfires and indicative of a firestorm, generating massive pyrocumulus. This could be the very reason why new index with atmospheric stability information captured better than the HDWI.

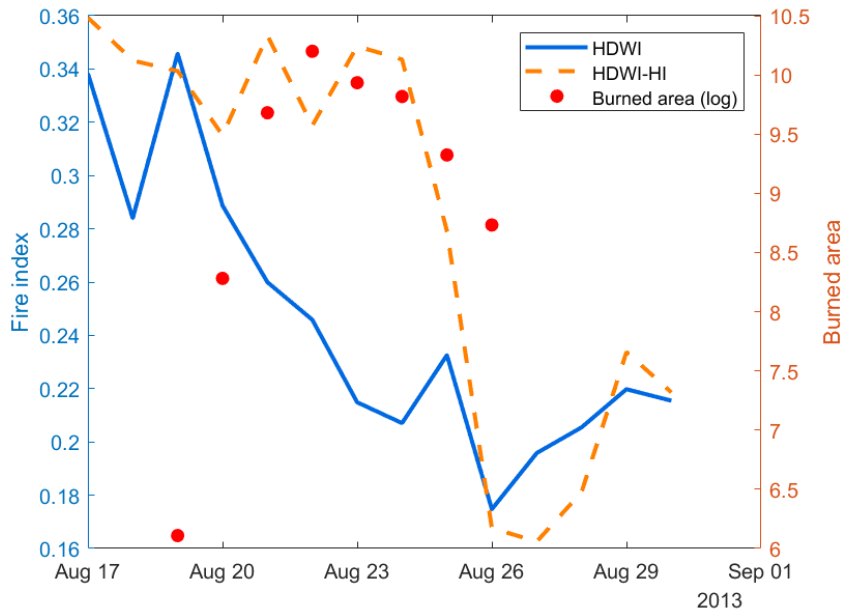

Figure 4.11 Case of Rim fire in 2013

Rim fire in 2013 is the best case to compare. The fire started on Aug 17 and the fire more than doubled to 53,887 acres overnight. Atmospheric instability, hot temperatures, and a severe drought fueled the fire, making it difficult to suppress. The new index captured the actual fire development well, especially after Aug 22. However, the HDWI index could not maintain the fire spread, mostly due to the lack inclusion of atmospheric instability.

4.4 Discussion and conclusion

This study provides a comprehensive evaluation of various fire weather indices across the western United States, focusing on their effectiveness in capturing wildfire occurrences over a 20-year period (2001-2020). Through meticulous data analysis using MODIS fire detections and a range of fire weather indices, the study reveals significant variations in index performance across different ecological regions.

Notably, indices like the Duff Moisture Code (DMC), Buildup Index (BUI), and the Fire Weather Index (FWI) show high reliability in regions such as the Rocky Mountains. In contrast, the hot-dry-windy index (HDWI) emerges as the top performer in Mediterranean California, highlighting the critical role of integrating wind variables in fire danger assessments in this region.

Further, the study introduces an innovative approach by combining the traditional fire indices with the Haines index, which assesses lower atmospheric stability and dryness. This new combined index, validated against large fire cases in California, demonstrates superior performance by incorporating atmospheric factors that significantly influence fire behavior. The findings underscore the importance of refining fire indices to include comprehensive meteorological data, which can enhance predictive accuracy and thus aid in more effective fire management strategies.

Overall, this research marks a significant step forward in understanding and improving fire danger ratings, potentially leading to more targeted and effective firefighting efforts in regions prone to wildfires. The study highlights the need for continuous adaptation of fire management tools to better address the dynamic nature of wildfire risks influenced by climate variability and change.

Chapter 5: Summary, future work and perspective

5.1 Summary

Our dissertation aims to deepen our comprehension of the climatic factors that drive wildfires in the western U.S. To address the scientific questions concerning the factors and mechanisms of increased wildfires, a lot of analyses have been conducted by making use of the rich dataset of fire, atmospheric and surface condition from satellite, ground observations and reanalysis data. This dissertation contributes to several aspects of the western U.S. wildfire studies:

The first study shed new light on the underlying regional climate processes affecting wildfire trends in NA and linkages with climate change under GHG warming. We provide observational evidence revealing physical relationships among wildfires in NA and regional feedback processes to changes in the large-scale circulation, global dryness, and linkages to GHG-induced warming. Results show that the western United States (WUS) has experienced the most robust increase in burned area, even though Alaska and western-central Canada have comparable warming trends. In addition to warming, the WUS has been under the influence of multi-decadal trends in tropospheric relative humidity deficit, reduced cloudiness, increased surface net insolation, and enhanced adiabatic warming and drying from increased tropospheric subsidence, as well as drying from enhanced offshore low-level flow. These trends are found to be associated with a widening of the descending branch of the Hadley circulation, consistent with climate model projections under greenhouse gases warming. Due to the

relative short (~30 years) data record, the aforementioned trend signals are likely also be affected by phase changes of natural interdecadal variability during the data period.

The second study of the dissertation focus on the analyzing the causes of the exceptional 2020 fire season in the western U.S. Our comprehensive examination shows this extraordinary year for fires in the western U.S is the result of "perfect storm", a combination of multiple climate and weather extremes. This unprecedented fire season was featured with August lightning-driven fires in California and September wind-driven fires in West Coast of U.S. The rare outbreak of CG lightning contributed most fire ignitions across northern California in August, while in September, majority fires are human ignited since the extreme high-pressure anomaly dominated over the entire western U.S, suppressing the development of storm and lightning activities. Both August and September were featured with extraordinary fuel aridity reflected by VPD, which enabled by climate and weather extremes, however, the mechanism of drying the fuel for these two months is different. In August, record high VPD is mainly contributed by record high surface temperature, while in September, record high pressure and sinking motion over the entire troposphere combined with high temperature contributed to the extreme VPD. To be noted, we found that dynamic related term contributed more than 50% to the deficit of tropospheric RH, indicating the importance of subsidence associated with atmospheric and surface dryness.

The third part of the dissertation evaluates the performance of the Canada and US fire indices over the various ecoregions of the western U.S. Results show that Canadian fire indices have better performance than the US fire indices in Mediterranean California and Western Cordillera in terms of conditional frequency cumulative

departure. US indices are more effective in the southwestern ecoregion including South Central semi-arid prairies, Upper Gila Mountain and Western Sierra Madre piedmont. VPD related group (VPD, VPD at 700 hPa and HDWI) show their effectiveness in terms of monthly correlation with active fire. With the surface wind information, hot and dry index ranks No.1 for the conditional frequency analysis over western costal region (Mediterranean California and Marine west coast forest), as these regions are featured with wind-driven fires. Feature importance rankings are consistent with the ranking from conditional frequency analysis over Mediterranean California and Western Cordillera ecoregions, both showing the best index is HDWI and DMC respectively. Results show that additional information from the lower troposphere (Haines index) further improves the performance of conditional frequency distribution over Mediterranean California and Western Cordillera ecoregions, suggesting the importance and usefulness of lower atmosphere stability and dryness in improving the predictive skill. Our case of several largest fires also exhibits the better skills for new combined index than the original HDWI over California, especially for these fires associated with the unstable atmosphere.

5.2 Contribution and Implications to Broader Wildfire Science Research

Our study firstly links the western U.S. large fires with the tropospheric drying associated with the multi-decadal trend of changes of Hadley circulation. The observational evidence emphasizes the importance of subsidence associated with tropospheric dryness. This work addresses a gap in the existing literature concerning the impact of anthropogenic climate warming on wildfire in the western U.S., While previous studies have documented the increasing frequency and severity of wildfires

associated with warming and drying, few have examined the direct link between anthropogenic climate change induced widespread tropospheric drying and the resulting changes in fuel aridity through the extended and enhanced descending component of Hadley circulation. The 2020 extraordinary fire season, particularly in September, serves as a compelling example of the critical significance of atmospheric dynamics to the surface and atmospheric RH deficit. It is anticipated that the frequency and severity of such high-pressure anomalies would increase due to greenhouse gas-induced warming, further exacerbating the occurrence of large fires in the western U.S.

"*From 1984 to 2015, about half of the increase in burned area across the western United States is attributable to increases in fuel flammability caused by anthropogenic climate change*", according to the Fifth National Climate Assessment in 2023. This revelation is a stark reminder of the significant impact our actions have on the environment, particularly in exacerbating the frequency and severity of wildfires. Such insight emphasizes the pressing need for robust mitigation and adaptation strategies to address climate change's repercussions. It highlights the importance of implementing measures to reduce greenhouse gas emissions, foster sustainable land management practices, and bolster community resilience to wildfires and other climate-related challenges.

Our refined new combined fire index introduces a novel and simple approach to quantifying wildfire risk by incorporating the lower atmospheric stability and dryness, which improves the predictive accuracy of the fire potential. This allows for more precise forecasting of wildfire occurrences and their potential severity, enabling better preparedness and response strategies for forest agencies. The refined fire index serves

as a valuable resource for fire management agencies, enabling them to allocate resources more effectively and implement targeted mitigation measures. This can lead to a significant reduction in wildfire damage and associated costs.

5.3 Limitations of the current study

Despite the general soundness of our observational evidence, we note their limitations in our current study. It is important to notice that the contribution of IPO may have confounded the climate and wildfire trends in our study. Separating the influence of GHG warming and multi-decadal internal variability requires a longer data period for burned areas and warrants future investigations.

For the 2020 fire study, it is still a major challenge to parse out the role of global warming (anthropogenic climate change) in driving this extraordinary fire year and a formal attribution is beyond the scope of our analysis, yet studies suggest that climate change implicated as a critical factor.

For the third study, the limited number of large fire case examinations is one of the limitations for the evaluation of the new combined fire index. In addition, interpretability and causality are the weaknesses of the random forest. It requires us to have a physical understanding of the parameters and feature rankings in the neural networks. Another major limitation is its suitability for certain types of large. While it is well-suited for wildfires that propagate under unstable atmospheric conditions, it may not be as effective for fires primarily driven by wind.

5.4 Future work

More investigations are suggested to address some of the limitations of this study mentioned above. It remains to be investigated whether RCFW is operative over other continental vegetated land regions (East Asia, Europe, South Africa, Australia, and South America) affected by global warming and atmospheric drying. If so, more wildfires on a global scale are likely to increase emissions of GHG and light-absorbing aerosols, such as black carbon and organic carbon, and these are also highly related to concerns of public health.

Future change of offshore winds and CG lightning would be critical for future fire in western U.S. For example, anthropogenic influences on climate may lead to a reduction in the frequency of offshore winds like the Santa Ana winds in Southern California due to uneven warming trends across continents. How these contrasting drivers work together with the increased drought and heat wave in the future merit further investigation.

More comprehensive global studies are required to explore the role of Vapor Pressure Deficit (VPD) in influencing global fire patterns. Additionally, it is imperative to investigate the feedback loop between increased large fires and the subsequent rise in CO2 emissions under anthropogenic warming.

Bibliography

Abatzoglou, J. T., & Williams, A. P. (2016). Impact of anthropogenic climate change on wildfire across western US forests. *Proceedings of the National Academy of Sciences USA*, *113*(42), 11,770–11,775. https://doi.org/10.1073/pnas.1607171113.

Abatzoglou, J. T., Williams, A. P., & Barbero, R. (2019). Global emergence of anthropogenic climate change in fire weather indices. *Geophysical Research Letters*, 46(1), 326–336. https://doi.org/10.1029/2018GL080959.

Abatzoglou, J. T., Kolden, C. A., Williams, A. P., Sadegh, M., Balch, J. K., & Hall, A. (2023). Downslope Wind‐Driven Fires in the Western United States. *Earth's Future*, 11(5), e2022EF003471.

Balch, J. K., Bradley, B. A., Abatzoglou, J. T., Nagy, R. C., Fusco, E. J., & Mahood, A. L. (2017). Human-started wildfires expand the fire niche across the United States. *Proceedings of the National Academy of Sciences USA*, 114(11), 2946–2951. https://doi.org/10.1073/pnas.1617394114.

Box, J. E., Colgan, W. T., Christensen, T. R., Schmidt, N. M., Lund, M., Parmentier, F.-J. W., … Skovgård Olsen, M. (2019). Key indicators of Arctic climate change: 1971–2017. *Environmental Research Letters*, 14(4), 045010. https://doi.org/10.1088/1748-9326/aafc1b.

Chiodi, A. M., Potter, B. E., & Larkin, N. K. (2021). Multi-decadal change in western US nighttime vapor pressure deficit. *Geophysical Research Letters*, 48(15),

Compo, G. P., Whitaker, J. S., Sardeshmukh, P. D., Matsui, N., Allan, R. J., Yin, X., … Worley, S. J. (2011). The Twentieth Century Reanalysis Project. *Quarterly Journal of the Royal Meteorological Society*, 137(654), 1–28. https://doi.org/10.1002/qj.776

Coop, J. D., Parks, S. A., Stevens-Rumann, C. S., Ritter, S. M., &Hoffman, C. M. (2022). Extreme fire spread events and area burned under recent and future climate in the western USA. *Global Ecology and Biogeography*,31(10), 1949-1959.

Dai, A. (2006). Recent climatology, variability, and trends in global surface humidity. *Journal of Climate*, 19(15), 3589–3606. https://doi.org/10.1175/JCLI3816.1.

Dai, A. (2011). Drought under global warming: a review. *Wiley Interdisciplinary Reviews: Climate Change*, 2(1), 45–65. https://doi.org/10.1002/wcc.81.

Dai, A. (2013). Increasing drought under global warming in observations and models. *Nature Climate Change*, 3, 52–58. https://doi.org/10.1038/nclimate1633.

Dai, A., & Zhao, T. (2017). Uncertainties in historical changes and future projections of drought. Part I: Estimates of historical drought changes. *Climatic Change*, 144, 519–533. https://doi.org/10.1007/s10584- 016-1705-2.

Dai, A., Trenberth, K. E., & Qian, T. (2004). A global dataset of Palmer drought severity index for 1870–2002: relationship with soil moisture and effects of surface warming. *Journal of Hydrometeorology*, 5(6), 1117–1130. https://doi.org/10.1175/JHM-386.

Dai, A., Zhao, T., & Chen, J. (2018). Climate change and drought: a precipitation and evaporation perspective. Current Climate Change Reports, 4, 301–312. https://doi.org/ 10.1007/s40641-018-0101-6.

Dee, D. P., Uppala, S. M., Simmons, A. J., Berrisford, P., Poli, P., Kobayashi, S., …. Vitart, F. (2011). The ERA-Interim reanalysis: configuration and performance of the data

assimilation system. Quarterly Journal of the Royal Meteorological Society, 137(656), 553–597. https://doi.org/10.1002/qj.828.

Dennison, P. E., Brewer, S. C., Arnold, J. D., & Moritz, M. A. (2014). Large wildfire trends in the western United States, 1984–2011. *Geophysical Research Letters*, 41(8), 2928–2933. https://doi.org/10.1002/2014GL059576.

Dong, B., & Dai, A. (2015). The influence of the interdecadal Pacific oscillation on temperature and precipitation over the globe. *Climate Dynamics*, 45(9-10), 2667–2681. https://doi.org/10.1007/s00382-015-2500-x.

Eidenshink, J. C., Schwind, B., Brewer, K., Zhu, Z.-L., Quayle, B., & Howard, S. M. (2007). A project for monitoring trends in burn severity. *Fire Ecology*, 3(1), 321. https://doi.org/10.4996/fireecology.0301003.

Fasullo, J. T., Otto‐Bliesner, B. L., & Stevenson, S. (2018). ENSO's changing influence on temperature, precipitation, and wildfire in a warming climate. *Geophysical Research Letters*, 45(17), 9216-9225.

Feng, S., & Fu, Q. (2013). Expansion of global drylands under a warming climate. *Atmospheric Chemistry and Physics*, 13(19), 10,081–10,094. https://doi.org/10.5194/acp-13-10081-2013.

Free, M., Sun, B., & Yoo, H. L. (2016). Comparison between total cloud cover in four reanalysis products and cloud measured by visual observations at U.S. weather stations. *Journal of Climate*, 29(6), 2015–2021. https://doi.org/10.1175/JCLI-D-15-0637.1.

Fu, Q., Manabe, S., & Johanson, C. M. (2011). On the warming in the tropical upper troposphere: models versus observations. *Geophysical Research Letters*, 38(15). https://doi.org/10.1029/2011GL048101.

Fu, R. (2015). Global warming-accelerated drying in the tropics. *Proceedings of the National Academy of Sciences USA,* 112(12), 3593. https://doi.org/10.1073/pnas.1503231112

Gelaro, R., McCarty, W., Suárez, M. J., Todling, R., Molod, A., Takacs, L., …. Zhao, B. (2017). The Modern-Era Retrospective Analysis for Research and Applications, Version 2 (MERRA-2). *Journal of Climate*, 30(14), 5419–5454.

Giglio, L., Justice, C., Boschetti, L., Roy, D. (2015). MCD64A1 MODIS/Terra+Aqua Burned Area Monthly L3 Global 500m SIN Grid V006 [Data set]. NASA EOSDIS Land Processes Distributed Active Archive Center. Accessed 2023-12-05 from https://doi.org/10.5067/MODIS/MCD64A1.006.

Guzman-Morales, J., & Gershunov, A. (2019). Climate change suppresses Santa Ana winds of southern California and sharpens their seasonality. *Geophysical Research Letters*, 46(5), 2772–2780. https://doi.org/10.1029/2018GL080261.

Harris, I., Osborn, T.J., Jones, P. et al. Version 4 of the CRU TS monthly high-resolution gridded multivariate climate dataset. Sci Data 7, 109 (2020). https://doi.org/10.1038/s41597-020-0453-3.

Harvey, B. J. (2016). Human-caused climate change is now a key driver of forest fire activity in the western United States. *Proceedings of the National Academy of Sciences USA*, 113(42), 11,649–11,650. https://doi.org/10.1073/pnas.1612926113.

Haines D A 1988 A lower atmospheric severity index for wildland fires Natl Weather Dig. 13 23–7.

Higuera, P. E., & Abatzoglou, J. T. (2020). Record-setting climate enabled the extraordinary 2020 fire season in the western United States. *Global change biology*, 27(1).

Holden, Z. A., Swanson, A., Luce, C. H., Jolly, W. M., Maneta, M., Oyler, J. W., …. Affleck, D. (2018). Decreasing fire season precipitation increased recent western US forest wildfire activity. *Proceedings of the National Academy of Sciences USA*, 115(36), E8349–E8357. https://doi.org/10.1073/pnas.1802316115.

Hu, Y., & Fu, Q. (2007). Observed poleward expansion of the Hadley circulation since 1979. *Atmospheric Chemistry and Physics*, 7(19), 5229–5236. https://doi.org/10.5194/acp-7-5229-2007.

Huang, J., Ji, M., Xie, Y., Wang, S., He, Y., & Ran, J. (2016). Global semi-arid climate change over last 60 years. *Climate Dynamics*, 46(3), 1131–1150.

Hughes, M., Hall, A., & Kim, J. (2011). Human-induced changes in wind, temperature and relative humidity during Santa Ana events. *Climatic Change*, 109(1), 119–132.

Jin, Y., Goulden, M. L., Faivre, N., Veraverbeke, S., Sun, F., Hall, A., …. Randerson, J. T. (2015). Identification of two distinct fire regimes in Southern California: implications for economic impact and future change. *Environmental Research Letters*, 10(9), 094005. https://doi.org/10.1088/1748-9326/10/9/094005.

Jain, P., Castellanos-Acuna, D., Coogan, S. C., Abatzoglou, J. T., & Flannigan, M. D. (2022). Observed increases in extreme fire weather driven by atmospheric humidity and temperature. *Nature ClimateChange*,12(1), 63-70.

Kalashnikov, D. A., Abatzoglou, J. T., Nauslar, N. J., Swain, D. L., Touma, D., & Singh, D. (2022). Meteorological and geographical factors associated with dry lightning in central and northern California. *Environmental Research: Climate*, 1(2), 025001.

Kanamitsu, M., Ebisuzaki, W., Woollen, J., Yang, S.-K., Hnilo, J. J., Fiorino, M., & Potter, G. L. (2002). NCEP–DOE AMIP-II Reanalysis (R-2). *Bulletin of the American*

Meteorological Society, 83(11), 1631–1644. https://doi.org/10.1175/BAMS-83-11-1631.

Kasischke, E. S., & Turetsky, M. R. (2006). Recent changes in the fire regime across the North American boreal region—Spatial and temporal patterns of burning across Canada and Alaska. *Geophysical Research Letters*, 33(9). https://doi.org/10.1029/2006GL025677

Kirchmeier-Young, M. C., Zwiers, F. W., Gillett, N. P., & Cannon, A. J. (2017). Attributing extreme fire risk in Western Canada to human emissions. *Climatic Change*, 144(2), 365–379. https://doi.org/10.1007/s10584-017-2030-0.

Kitzberger, T., Brown, P. M., Heyerdahl, E. K., Swetnam, T. W., & Veblen, T. T. (2007). Contingent Pacific–Atlantic Ocean influence on multicentury wildfire synchrony over western North America. *Proceedings of the National Academy of Sciences USA*, 104(2), 543–548. https://doi.org/10.1073/pnas.0606078104.

Kobayashi, S., Ota, Y., Harada, Y., Ebita, A., Moriya, M., Onoda, H., …. Takahashi, K. (2015). The JRA-55 reanalysis: general specifications and basic characteristics. *Journal of the Meteorological Society of Japan*. Ser. II, 93(1), 5–48.

Lau, W. K. M., Wu, H.-T., & Kim, K.-M. (2013). A canonical response of precipitation characteristics to global warming from CMIP5 models. *Geophysical Research Letters*, 40(12), 3163–3169. https://doi.org/10.1002/grl.50420.

Lau, W. K. M., & Kim, K.-M. (2015). Robust Hadley circulation changes and increasing global dryness due to CO2 warming from CMIP5 model projections. *Proceedings of the National Academy of Sciences USA*, 201418682.

Lau, W. K. M., & Kim, K.-M. (2017). Competing influences of greenhouse warming and aerosols on Asian summer monsoon circulation and rainfall. Asia-Pacific *Journal of Atmospheric Sciences*, 53(2), 181–194. https://doi.org/10.1007/s13143-017-0033-4,

Lau, W. K., &Tao, W. (2020). Precipitation–radiation–circulation feedback processes associated with structural changes of the ITCZ in a warming climate during 1980–2014: An observational portrayal. *Journal of Climate*,33(20), 8737-8749.

Littell, J. S., McKenzie, D., Peterson, D. L., & Westerling, A. L. (2009). Climate and wildfire area burned in western U.S. ecoprovinces, 1916–2003. *Ecological Applications*, 19(4), 1003–1021. https://doi.org/10.1890/07-1183.1.

Littell, J. S., Peterson, D. L., Riley, K. L., Liu, Y., & Luce, C. H. (2016). A review of the relationships between drought and forest fire in the United States. *Global Change Biology*, 22(7), 2353–2369. https://doi.org/10.1111/gcb.13275.

Liu, Y., Stanturf, J., & Goodrick, S. (2010). Trends in global wildfire potential in a changing climate. *Forest Ecology and Management*, 259(4), 685–697.

Liu, Y., Goodrick, S., & Heilman, W. (2014). Wildland fire emissions, carbon, and climate: Wildfire–climate interactions. *Forest Ecology and Management*, 317, 80–96. https://doi.org/10.1016/j.foreco.2013.02.020.

Lorenz, D. J., & DeWeaver, E. T. (2007). Tropopause height and zonal wind response to global warming in the IPCC scenario integrations. *Journal of Geophysical Research: Atmospheres*, 112(D10). https://doi.org/10.1029/2006JD008087.

Lu, J., Vecchi, G. A., & Reichler, T. (2007).Expansion of the Hadley cell under global warming *Geophysical Research Letters*, 34(6). https://doi.org/10.1029/2006GL028443.

Miller, N. L., & Schlegel, N. J. (2006). Climate change projected fire weather sensitivity: California Santa Ana wind occurrence. *Geophysical Research Letters*, 33(15). https://doi.org/10.1029/2006GL025808.

Pan, X., Chin, M., Ichoku, C. M., & Field, R. D. (2018). Connecting Indonesian fires and drought with the type of El Niño and phase of the Indian Ocean dipole during 1979–2016. *Journal of Geophysical Research: Atmospheres*, 123(15), 7974–7988. https://doi.org/10.1029/2018JD028402.

Picotte, J. J., Peterson, B. E., Meier, G., & Howard, S. M. (2016). 1984–2010 trends in fire burn severity and area for the conterminous US. *International Journal of Wildland Fire*, 25(4), 413420. https://doi.org/10.1071/WF15039.

Pinto, M. M., DaCamara, C. C., Hurduc, A., Trigo, R. M., & Trigo, I. F. (2020). Enhancing the fire weather index with atmospheric instability information. *Environmental Research Letters*, 15(9), 0940b7.

Rossow, W. B., & Schiffer, R. A. (1991). ISCCP Cloud Data Products. *Bulletin of the American Meteorological Society*, 72(1), 2–20. https://doi.org/10.1175/1520-0477(1991)072<0002:ICDP>2.0.CO;2.

Russell, E. N., Loikith, P. C., Ajibade, I., Done, J. M., & Lower, C. (2024). The meteorology and impacts of the September 2020 Western United States extreme weather event. *Weather and Climate Extremes*, 43, 100647.

Running, S. W. (2006). Climate Change: Is global warming causing more, larger wildfires? *Science*, 313(5789), 927–928. https://doi.org/10.1126/science.1130370.

Santer, B. D., Thorne, P. W., Haimberger, L., Taylor, K. E., Wigley, T. M. L., Lanzante, J. R., … Wentz, F. J. (2008). Consistency of modelled and observed temperature trends in

the tropical troposphere. *International Journal of Climatology*, 28(13), 1703–1722. https://doi.org/10.1002/joc.1756.

Santer, Benjamin D., Solomon, S., Pallotta, G., Mears, C., Po-Chedley, S., Fu, Q., Bonfils, C. (2016). Comparing tropospheric warming in climate models and satellite data. *Journal of Climate*, 30(1), 373–392. https://doi.org/10.1175/JCLI-D-16-0333.1.

Santos, L. C., Lima, M. M., Bento, V. A., Nunes, S. A., DaCamara, C. C., Russo, A., ... & Trigo, R. M. (2023). An Evaluation of the Atmospheric Instability Effect on Wildfire Danger Using ERA5 over the Iberian Peninsula. *Fire*, 6(3), 120.

Safford, H. D., Paulson, A. K., Steel, Z. L., Young, D. J., & Wayman, R. B. (2022). The 2020 California fire season: A year like no other, a return to the past or a harbinger of the future?. *Global Ecology and Biogeography*, 31(10), 2005-2025.

Schoennagel, T., Veblen, T. T., Romme, W. H., Sibold, J. S., & Cook, E. R. (2005). ENSO and PDO variability affect drought-induced fire occurrence in Rocky Mountain subalpine forests. *Ecological Applications*, 15(6), 2000–2014. https://doi.org/10.1890/04-1579.

Seager, R., & Vecchi, G. A. (2010). Greenhouse warming and the 21st century hydroclimate of southwestern North America. *Proceedings of the National Academy of Sciences USA*, 107(50), 21,277–21,282. https://doi.org/10.1073/pnas.0910856107.

Seager, R., Hooks, A., Williams, A. P., Cook, B., Nakamura, J., & Henderson, N. (2015). Climatology, variability, and trends in the US vapor pressure deficit, an important fire-related meteorological quantity. *Journal of Applied Meteorology and Climatology*, 54(6), 1121–1141. https://doi.org/10.1175/JAMC-D-14-0321.1.

Seidel, D. J., & Randel, W. J. (2007). Recent widening of the tropical belt: evidence from tropopause observations. *Journal of Geophysical Research: Atmospheres*, 112(D20). https://doi.org/10.1029/2007JD008861.

Seidel, D. J., Fu, Q., Randel, W. J., & Reichler, T. J. (2008). Widening of the tropical belt in a changing climate. *Nature Geoscience*, 1(1), 21–24.

Sherwood, S. C., Ingram, W., Tsushima, Y., Satoh, M., Roberts, M., Vidale, P. L., & O'Gorman, P. A. (2010). Relative humidity changes in a warmer climate. *Journal of Geophysical Research: Atmospheres*, 115(D9). https://doi.org/10.1029/2009JD012585

Smith, A., Lott, N., & Vose, R. (2011). The Integrated Surface Database: recent developments and partnerships. *Bulletin of the American Meteorological Society*, 92(6), 704–708. https://doi.org/10.1175/2011BAMS3015.1.

Srock, A. F., Charney, J. J., Potter, B. E., & Goodrick, S. L. (2018). The hot-dry-windy index: A new fire weather index. *Atmosphere*, 9(7), 279.

Stuivenvolt Allen, J., Simon Wang, S. Y., LaPlante, M. D., & Yoon, J. H. (2021). Three Western Pacific typhoons strengthened fire weather in the recent northwest US conflagration. *Geophysical Research Letters*, 48(3), e2020GL091430.

Sun, B., Free, M., Yoo, H. L., Foster, M. J., Heidinger, A., & Karlsson, K.-G. (2015). Variability and trends in U.S. cloud cover: ISCCP, PATMOS-x, and CLARA-A1 compared to homogeneity-adjusted weather observations. *Journal of Climate*, 28(11), 4373–4389. https://doi.org/10.1175/JCLI-D-14-00805.1.

Veblen, T. T., Kitzberger, T., & Donnegan, J. (2000). Climatic and human influences on fire regimes in Ponderosa pine forests in the Colorado Front Range. *Ecological Applications*, 10(4), 1178–1195.

Veraverbeke, S., Rogers, B. M., Goulden, M. L., Jandt, R. R., Miller, C. E., Wiggins, E. B., & Randerson, J. T. (2017). Lightning as a major driver of recent large fire years in North American boreal forests. *Nature Climate Change*, 7(7), 529–534.

Wang, S., Huang, J., He, Y., & Guan, Y. (2014). Combined effects of the Pacific Decadal Oscillation and El Niño-Southern Oscillation on global land dry-wet changes. *Scientific Reports*, 4, 6651. https://doi.org/10.1038/srep06651.

Westerling, A. L., Gershunov, A., Brown, T. J., Cayan, D. R., & Dettinger, M. D. (2003). Climate and wildfire in the western United States. *Bulletin of the American Meteorological Society*, 84(5), 595–604. https://doi.org/10.1175/BAMS-84-5-595.

Westerling, A. L., Hidalgo, H. G., Cayan, D. R., & Swetnam, T. W. (2006). Warming and earlier spring increase western U.S. f*orest* wildfire activity. *Science*, 313(5789), 940–943. https://doi.org/10.1126/science.1128834.

Wild, M. (2011). Enlightening global dimming and brightening. *Bulletin of the American Meteorological* Society, 93(1), 27–37. https://doi.org/10.1175/BAMS-D-11-00074.1

Willett, K. M., Dunn, R. J. H., Thorne, P. W., Bell, S., de Podesta, M., Parker, D. E., … Williams Jr., C. N. (2014). HadISDH land surface multi-variable humidity and temperature record for climate monitoring. *Climate of the Past*, 10(6), 1983–2006. https://doi.org/10.5194/cp-10-1983-2014.

Williams, A. P., Seager, R., Berkelhammer, M., Macalady, A. K., Crimmins, M. A., Swetnam, T. W., …. Rahn, T. (2014). Causes and implications of extreme atmospheric moisture demand during the record-breaking 2011 wildfire season in the southwestern United States. *Journal of Applied Meteorology and Climatology*, 53(12), 2671–2684. https://doi.org/10.1175/JAMC-D-14-0053.1.

Wuebbles, D. (2017). Climate Science Special Report: Fourth National Climate Assessment (NCA4), Volume I | GlobalChange.gov. Retrieved September 25, 2019, from https://www.globalchange.gov/browse/reports/climate-science-special-report-fourth-national-climate-assessment-nca4-volume-i.

Yin, J. H. (2005). A consistent poleward shift of the storm tracks in simulations of 21st century climate. *Geophysical Research Letters*, 32(18). https://doi.org/10.1029/2005GL02368.

Yue, X., Mickley, L. J., & Logan, J. A. (2014). Projection of wildfire activity in southern California in the mid-twenty-first century. *Climate Dynamics*, 43(7), 1973–1991. https://doi.org/10.1007/s00382-013-2022-3.

Zhao, T., & Dai, A. (2017). Uncertainties in historical changes and future projections of drought. Part II: Model-simulated historical and future drought changes. Climatic Change, 144(3), 535–548. https://doi.org/10.1007/s10584-016-1742-x.

Zhang, L., Lau, W., Tao, W., & Li, Z. (2020). Large wildfires in the Western United States exacerbated by tropospheric drying linked to a multi-decadal trend in the expansion of the Hadley circulation. *Geophysical Research Letters*, 47(16), e2020GL087911.

Zhuang, Y., Fu, R., Santer, B. D., Dickinson, R. E., & Hall, A. (2021). Quantifying contributions of natural variability and anthropogenic forcings on increased fire weather risk over the western United States. *Proceedings of the National Academy ofSciences*,118(45), e2111875118.

Ziel, R. H., Bieniek, P. A., Bhatt, U. S., Strader, H., Rupp, T. S., & York, A. (2020). A comparison of fire weather indices with MODIS fire days for the natural regions of Alaska. *Forests*, 11(5), 516.